بسم الله الرحمن الرحيم

Sudan University of Science and Technology

College of Graduate Studies

School of Electrical and Nuclear Engineering

Impact of UPFC on Sudanese National Grid

تأثير متحكمة سريان القدرة الموحدة على شبكة الكهرباء السودانية

A Thesis submitted in partial fulfillment for the requirement of the degree of M.Sc. in Electrical Engineering (Power)

Prepared by:

Mohammed Mirghani Hassan

Supervisor:

Dr. Mohamed Osman Hassan

Feb 2016

الآيـــــة

﴿ أَلَمْ تَرَوْا أَنَّ اللَّهَ سَخَّرَ لَكُمْ مَا فِي السَّمَاوَاتِ وَمَا فِي الْأَرْضِ وَأَسْبَغَ عَلَيْكُمْ نِعَمَهُ ظَاهِرَةً وَبَاطِنَةً وَمِنَ النَّاسِ مَنْ يُجَادِلُ فِي اللَّهِ بِغَيْرِ عِلْمٍ وَلَا هُدًى وَلَا كِتَابٍ مُنِيرٍ * وَإِذَا قِيلَ لَهُمُ اتَّبِعُوا مَا أَنْزَلَ اللَّهُ قَالُوا بَلْ نَتَّبِعُ مَا وَجَدْنَا عَلَيْهِ آبَاءَنَا أَوَلَوْ كَانَ الشَّيْطَانُ يَدْعُوهُمْ إِلَى عَذَابِ السَّعِيرِ * وَمَنْ يُسْلِمْ وَجْهَهُ إِلَى اللَّهِ وَهُوَ مُحْسِنٌ فَقَدِ اسْتَمْسَكَ بِالْعُرْوَةِ الْوُثْقَى وَإِلَى اللَّهِ عَاقِبَةُ الْأُمُورِ * وَمَنْ كَفَرَ فَلَا يَحْزُنْكَ كُفْرُهُ إِلَيْنَا مَرْجِعُهُمْ فَنُنَبِّئُهُمْ بِمَا عَمِلُوا إِنَّ اللَّهَ عَلِيمٌ بِذَاتِ الصُّدُورِ* ﴾

لقمان (20 - 23)

DEDICATION

I heartily dedicate this piece of work to:

My mother who taught me that even the largest task can be accomplished if it is done one step at a time.

My father who taught me that the best kind of knowledge to have is that which is learned for its own sake.

My Friends who have encouraged me to complete this work.

My classmates who have supported me by good ideas throughout the research.

Other honest researchers who have the ability to push this article furthermore.

ACKNOWLEDGEMENT

First of all, thanks Allah for guiding me to perform this thesis, otherwise all works will not be completed except with his blessing. I would like to express my profound gratitude to my advisor **Dr. Mohammed Osman Hassan** for his invaluable advice and continuous encouragement throughout this work. His suggestions provide me the opportunity to instruct and solve the faced problems. I would also thank him for providing the commercial NEPLAN software.

I would like to thank my superior fellow Eng. Abdelrahman Elrayh Makki who is encouraging me by his strength and intelligence to work hard and complete this thesis. I am also thankful to my friend and classmate Eng. Abdelilah Dafa'allah for his valuable suggestions and discussions.

A special thank to my intimate M.Sc. fellows at SUST: M.Alhadi, O.Basher. I enjoyed every moment working together in the theoretical period. Many thanks to my close Bachelor classmates for their encouragement.

It is impossible to find the right words to thank my beloved parents, my two brothers and my sister for their love and encouragement. Without it, this thesis would not be completed.

ABSTRACT

The problem of improving the voltage profile and reducing power losses in electrical networks is a task that must be solved in an optimal manner. Therefore, placement of FACTS devices in suitable location to control the line flow and maintain bus voltages in a desired level and reduce losses is required. The unified power flow controller (UPFC) is able to control, concurrently or selectively, all transmission line parameters, voltage, impedance, and angle.

The overall aim of the research is to enhance the voltage profile and reduce power losses in Sudanese electrical network, this thesis presents one of the voltage stability indices i.e. a line stability index L_{mn} which is used to seek the optimal location of FACTS devices in a power system. Proposed algorithm is applied on Sudanese electrical network for optimally installing multi UPFC devices in the system. Optimal power flow (OPF) has been utilized to set the power flow parameters for the UPFC.

Seven UPFC devices are optimally installed in the system, the overall voltage profile is improved and confined within $\pm 5\%$ and total active and reactive losses of the system have been decreased by 6.96% and 0.74% of the base case, respectively. Results are obtained using NEPLAN software.

المستخلص

مشكلة تحسين الجهود وتقليل الفقودات في الشبكة الكهربائية يجب حلها بأفضل أسلوب علمي، لذلك فإن تركيب الأنظمة المرنة لنقل الكهرباء (FACTS) في موضعها الأمثل للتحكم في سريان القدرة الكهربية وتحسين الجهود وتقليل الفقودات أمر لابد منه. متحكمة سريان القدرة الموحدة (UPFC) باستطاعتها التحكم في جميع العوامل المؤثرة في نقل القدرة الكهربائية (الجهد، المعاوقة، زاوية القدرة) في نفس الوقت أو بصورة انتقائية.

الهدف من هذه الدراسة هو تحسين الجهود وتقليل الفقودات الكهربائية في شبكة الكهرباء السودانية. هذه الدراسة توضح أحد مؤشرات استقرارية الجهد الكهربي وهو مؤشر استقرارية الخطوط (L_{mn}) الذي يستخدم في إيجاد المكان الأمثل في الشبكة الكهربائية لتركيب أجهزة الـ (FACTS). تم تطبيق الخوارزمية المقترحة علي شبكة الكهرباء السودانية لتركيب عدد من أجهزة الـ (UPFC) في الشبكة بصورة مثلى. و بالاستفادة من مخطط سريان القدرة الأمثل (OPF) تم تحديد معاملات القدرة لأجهزة الـ (UPFC).

تم تركيب سبعة من أجهزة الـ (UPFC) بصورة مثلى في الشبكة، مما أدى إلى تحسين الشكل العام للجهد في الشبكة حتى أصبحت كل الجهود محدودة في سماحية $\pm 5\%$، و قلت الفقودات في القدرة الفعلية والردفعلية بمقدار 6.96% و 0.74% على التوالي. تم الحصول على النتائج باستخدام برنامج NEPLAN.

CONTENTS

الآيـــــة…… i

DEDICATION…… ii

ACKNOWLEDGEMENT…… iii

ABSTRACT…… iv

المستخلص…… v

LIST OF FIGURES…… viii

LIST OF TABLES…… ix

ABBREVIATIONS…… x

1 INTRODUCTION

1.1 Introduction…… 1

1.2 Literature review…… 1

1.3 Statement of problem…… 3

1.4 Thesis objectives…… 3

1.5 Methodology…… 4

1.6 Thesis outline …… 4

2 CONCEPTS OF FACTS CONTROLLERS

2.1 Introduction…… 5

2.2 Flexible AC Transmission Systems…… 6

2.3 FACTS controllers' classification regarding to the power electronic devices used in the control operation…… 7

2.3.1 Thyristor based FACTS devices…… 7

2.3.2 Voltage source converter based FACTS devices…… 8

2.4 FACTS controllers' classification regarding to their connection in the network…… 9

2.5 FACTS devices benefits…… 10

2.6 Power electronic controllers based on fully controlled semiconductor devices…… 12

2.6.1 Voltage source converter…… 14

2.6.2 Principles of voltage source converter operation…… 15

2.6.3 Control capabilities of controllers based on voltage source converters……..……. 17
2.7 The unified power flow controller……...…..… 18
2.7.1 The static compensator…….…..….. 18
2.7.2 The solid state series compensator……..…..……... 20
2.7.3 Basic principle of UPFC operation……..……. 23
3 PLACEMENT STRATEGY OF UPFC
3.1 Introduction……..…….. 27
3.2 Optimal location for UPFC……..…….. 27
3.2.1 Line stability index (L_{mn}) calculation…….…….…… 28
3.3 UPFC parameter setting……..……... 31
3.4 Criteria for optimal location of UPFC……...……... 32
3.5 Software developments……..…… 34
3.5.1 Description of UPFC in NEPLAN…….…….. 34
4 SIMULATION AND RESULTS
4.1 Sudanese electrical network……..……. 36
4.2 Optimal locations for UPFC devices…...……..…… 45
4.3 System improvements after installing the UPFC devices……..…… 50
5 CONCLUSION AND RECOMMENDATIONS
5.1 Conclusion……..……... 62
5.2 Recommendations……..…… 63
REFERENCES…...…… 64
APPENDICES.....…….…….. 67

LIST OF FIGURES

Figure No	Title	Page No
2.1	Group of conventional thyristor-controlled FACTS controllers……...	8
2.2	Group of voltage-sourced converter-based FACTS controllers……...	8
2.3	FACTS controller's classifications based on their connection in the network..	9
2.4	Circuit symbols for GTO and IGPT……..	12
2.5	Topology of a three-phase, two-level voltage source converter VSC...……	14
2.6	Basic operation of a voltage source converter VSC...……..	15
2.7	Phasor diagram illustrating the general concept of VSC control……..	18
2.8	Static compensator (STATCOM) system……..	19
2.9	Solid state series compensator (SSSC) system……..	21
2.10	Unified power flow controller (UPFC) system……..	22
2.11	Unified power flow controller equivalent circuit…….....	23
3.1	Two bus system…….	28
3.2	Flow chart of the proposed approach…….	33
3.3	Schematic symbol of UPFC in NEPLAN……..	34
4.1	Single line diagram of Sudanese electrical network ……...……..	37
4.2	Busses near to the lower limit……...…….	42
4.3	Voltage profiles at base case…….	43
4.4	Active power at base case…….	43
4.5	Reactive power at base case……..	43
4.6	Percentage loading at base case…….	44
4.7	Active power losses at base case……...	44
4.8	Reactive power losses at base case……	44
4.9	Voltage profiles with and without UPFC's……	54
4.10	Voltage improvements at the weak busses……	54
4.11	Active power with and without UPFC's……	55
4.12	Reactive power with and without UPFC's……	56
4.13	Percentage loading with and without UPFC's……...	56
4.14	Active power losses with and without UPFC's…….	57
4.15	Reactive power losses with and without UPFC's……..	58
4.16	Total active power loss……..	59
4.17	Total reactive power loss……...	59
4.18	Total saved power and percentage improvement……..	59
4.19	Voltage profiles according to number of UPFC devices installed…….	60
4.20	Active power losses according to number of UPFC devices installed……..	61
4.21	Reactive power losses according to number of UPFC devices installed……...	61

LIST OF TABLES

Table No	Title	Page No
2.1	Overview of major FACTS devices…….	10
2.2	The role of FACTS controllers in power system operation…….	11
3.1	UPFC parameters…….	35
4.1	Bus voltage and angle at base case……..	38
4.2	Power flow results at base case……	40
4.3	Line stability index with system loading…….	45
4.4	Ranking of lines severity……..	48
4.5	Selected places for UPFC installation …….	49
4.6	Parameters of installed UPFC's……...	49
4.7	Bus voltage and angle after installing UPFC devices……..	50
4.8	Power flow results after installing UPFC devices……...	52
4.9	Power flow improvement…….	58
4.10	Power flow improvement according to number of UPFC devices installed……...	60

ABBREVIATIONS

AC	Alternating Current.
FACTS	Flexible AC Transmission System.
UPFC	Unified Power Flow Controller.
HVDC	High Voltage Direct Current.
SVC	Static VAR Compensators.
IGBT	Insulated Gate Bipolar Transistor.
GTO	Gate Turn-Off thyristor.
PSAT	Power System Analysis Toolbox.
VSC	Voltage Source Converter.
TCVR	Thyristor Controlled Voltage Regulators.
TCPAR	Thyristor Controlled Phase Angle Regulators.
STATCOM	Static Synchronous Compensator.
SSSC	Static Synchronous Series Compensator.
IPFC	Interline Power Flow Controller.
TCR	Thyristor Controlled Reactor.
PS	Phase Shifter.
V_x	Voltage drop across reactor.
V_s	Supply voltage.
$V_{vR}\angle\delta_{vR}$	Voltage magnitude and angle of shunt converter.
$V_{cR}\angle\delta_{cR}$	Voltage magnitude and angle of series converter.
$I_m\angle\gamma_m$	Line current magnitude and angle.
LTC	Load Tap Changer.
VSI	Voltage Stability Index.
VCPI	Voltage Collapse Point Indicators.
L_{mn}	Line stability index.
FVSI	Fast Voltage Stability Index.
CPF	Continuation Power Flow.
OPF	Optimal Power Flow.
I_q	Current injected by the shunt converter.
R	Line resistance.
X	Line reactance.
Z	Line impedance.
G	Line conductance.
B	Line susceptance.
θ	Line impedance angle.
P	Active power MW.
Q	Reactive power MVAr.
GUI	Graphical User Interface.

CHAPTER ONE

INTRODUCTION

1.1 Introduction

The main aim of a modern electrical power system is to satisfy continuously the electrical power contracted by all customers. This is a problem of great engineering complexity where the following operational policies must be observed: (1) nodal voltage magnitudes and system frequency must be kept within narrow boundaries; (2) the alternating current (AC) voltage and current waveforms must remain largely sinusoidal; (3) transmission lines must be operated well below their thermal and stability limits; and (4) even short-term interruptions must be kept to a minimum. Moreover, because of the very competitive nature of the electricity supply business in an era of deregulation and open access, transmission costs must be kept as low as possible [1].

1.2 Literature review

The rapid development of the power electronics technology provides opportunities to develop new power equipment to improve the performance of the power system. Power electronics was first applied in power systems compensation with the advent of power semiconductor diodes and thyristors in the 1970s. Among the first applications were High Voltage DC (HVDC) transmission systems, based on thyristor rectifiers and inverters [2], The

various thyristor circuits used to generate and control the reactive power [4 - 6]. These technologies have been instrumental in the broad application of high voltage DC and AC transmissions. They have already made a significant impact on AC transmission via the increasing use of thyristor controlled static VAR compensators (SVCs).

The advancement of power semiconductor devices such as the Insulated Gate Bipolar Transistor (IGBT) and the Gate Turn-Off thyristor (GTO) which possess high power handling capability have led the development of controllable reactive power sources utilizing electronic switching converter technology [8]. The UPFC is the one of most powerful FACTS devices, introduced by L.Gyugyi. Various mathematical model of UPFC has been introduced depend upon various purpose of application [1, 2, 3, and 9].

Different approaches have been applied to increase the stability and security of power systems, over the last few decades, by improving voltage profiles, minimizing losses and minimizing operational power factor. For the Power system static performance studies the UPFC power injection model is introduced [2, 4]. The UPFC injection model has implemented into a full Newton-Raphson program by adding the UPFC power injections model and by derivatives the elements of jacobian matrix with respect to the AC network state variables. An effective placement strategy for UPFC is proposed in [10, 12 and 14]. The method uses Line stability index which is sensitive to line flow to screen down the possible locations for UPFC.

The steady-state models of the FACTS controllers produced algebraic equations which were combined with power system network algebraic equations and these were solved using Newton-Raphson solution technique is presented in [22]. The selection of the best possible location for

installation of SVC and UPFC is carried out with an objective of reducing the losses and improving the voltage using PSAT in [23].

1.3 Statement of problem

Day by day all over the world the demand of electric power is increasing. Not only that, the demand of power by the consumer is more than the power flowing through the transmission line. In order to provide the power that achieved the consumers demand the FACTS technology introduced. The maximum loads which are used in daily life or industrial purpose are inductive type. This type of load are consumed the reactive power. To control and regulate the active and reactive power the various FACTS device are used. The UPFC is most promising device among the entire FACTS device. The UPFC can control transmission voltage, impedance, and phase angle. The UPFC can also enhance the active and reactive power capacity of the system.

1.4 Thesis objectives

The objectives of the research are:

1. To study the basic operation of UPFC; to study the model of UPFC and how it can be operated in the system.
2. To analyze the impact of UPFC in the transmission line; to improve voltage profile and reduce transmission power losses by incorporating UPFC, Sudanese power grid will be tested.
3. To install the sufficient number of UPFC devices in the system at their optimal locations.

1.5 Methodology

The method for optimal UPFC placement where the objective is to minimize the line losses and the bus voltage limit violations is proposed. The method is implemented on Sudanese electrical network. The optimal locations are achieved by using the line stability index L_{mn} at heavy active and reactive power loading. The line having the highest value of L_{mn} is considered the best location for UPFC, followed by other lines having less value.

To push the system toward its optimal power flow profile, OPF results is used to set the power flow parameters for the UPFC.

Seven UPFC devices are installed in the system one by one and the system improvements are compared with the previous case until there is no improvement considered. NEPLAN software is used to simulate the system and obtain the power flow results.

1.6 Thesis outlines

This thesis consists of five chapters. Chapter two gives brief description for various FACTS controllers, and then represents a full discussion on UPFC, its model, control capabilities and operating principles. The placement strategy of UPFC devices at the optimal locations in Sudanese electrical network is described in chapter three. Chapter four gives a discussion on the improvement in voltage profile and transmission power losses in the network and these results are compared with base case results. At the end conclusions and scope of future work is given in chapter five.

CHAPTER TWO

CONCEPTS OF FACTS CONTROLLERS

2.1 Introduction

The concept of FACTS and FACTS controllers was first defined by Hingorani in 1988 [3], FACTS is defined as 'Alternating current transmission systems incorporating power electronic-based and other static controllers to enhance controllability and increase power transfer capability'. The FACTS controller is defined as 'a power electronic based system and other static equipment that provide control of one or more AC transmission system parameters' [3, 4].

FACTS controllers used to control the power flow and enhance stability, and they have become, not only common words in the power industry, but they have started replacing many mechanical control devices. They are certainly playing an important and a major role in the operation and control of modern power systems [3], FACTS devices provide new control facilities, both in steady state power flow and dynamic stability control [5].

The potential benefits brought about by FACTS controllers include reduction of operation and transmission investment cost, increased system security and reliability, increased power transfer capabilities, and an overall enhancement of the quality of the electric energy delivered to customers [1].

The capital investment and the operating costs (essentially the cost of power losses and maintenance) are offset against the benefits provided by the FACTS controllers, and it is important to ascertain the major issues in the

deployment of FACTS controllers which are the location, ratings and control strategies required for the optimal utilization [4].

2.2 Flexible AC Transmission Systems

The FACTS initiative was originally launched to solve the emerging problems faced due to restrictions on transmission line construction, and to facilitate growing power export/import and wheeling transactions among utilities. The two basic objectives behind the development of FACTS technology are to increase the power transfer capability of transmission systems, and to keep the power flowing over designated routes [2], therefore significantly increasing the utilization of existing and new transmission assets. This plays a major role in facilitating contractual power flow in electricity markets with minimal requirements for new transmission lines.

Injecting a series voltage phasor, with a desirable voltage magnitude and phase angle in a line, can provide a powerful means of precisely controlling the active and reactive power flows, by which, system stability can be improved, system reliability can be enhanced while operating and transmission investment cost can be reduced. It is possible to vary the impedance of a specific transmission line to force power flow along a desired “contract path” in the emerging power systems, to regulate the unwanted loop power flows and parallel power flows in the interconnected system. Dynamic reactive power compensation and damping power system oscillations can also be achieved using FACTS controllers.

FACTS controllers are classified regarding to two considerations:

- Regarding to the power electronic devices used in the control operation.
- Regarding to their connection in the network.

2.3 FACTS controllers' classification regarding to the power electronic devices used in the control operation

Depending on the power electronic devices used in the control, the FACTS controllers can be classified as:

- Thyristor based FACTS devices.
- Voltage source converter (VSC) based FACTS devices.

2.3.1 Thyristor based FACTS devices

This group employs reactive impedances and tap-changing transformers with conventional thyristor valves (switches) as controlled elements. This group, the Static Var Compensator (SVC), Thyristor-Controlled Series Capacitor, and Thyristor-Controlled Voltage and Phase Angle Regulators (TCVR and TCPAR) as illustrated in figure 2.1, is similar in circuit configuration to the breaker-switched capacitors, reactors and mechanical tap-changing transformers, but have a much faster response and are operated by sophisticated controls [3].

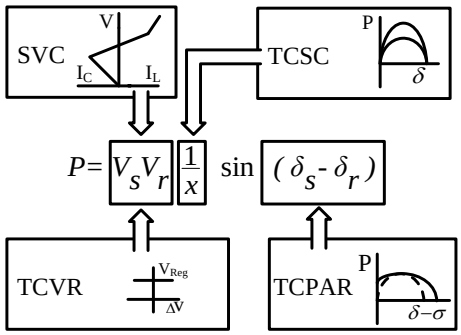

Figure 2.1: Group of conventional thyristor-controlled FACTS controllers.

2.3.2 Voltage source converter based FACTS devices

This group employs self-commutated, voltage-sourced switching converters to realize rapidly controllable, static synchronous voltage sources. The operation and performance of this group, as illustrated in figure 2.2, include the Static Synchronous Compensator (STATCOM), Static Synchronous Series Compensator (SSSC), and the Static Synchronous Voltage and Angle Regulators, are analogous to those characterizing ideal synchronous machines, providing almost instantaneous speed of response and control characteristics which are independent of system voltage (shunt operation) and current (series operation) [3].

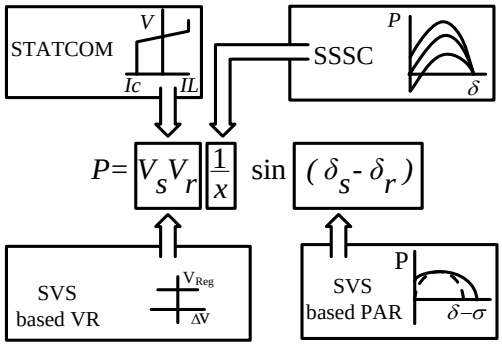

Figure 2.2: Group of voltage-sourced converter-based FACTS controllers.

2.4 FACTS controllers' classification regarding to their connection in the network

FACTS controllers can be divided into four categories based on their connection in the network, figure 2.3 shows these categories.

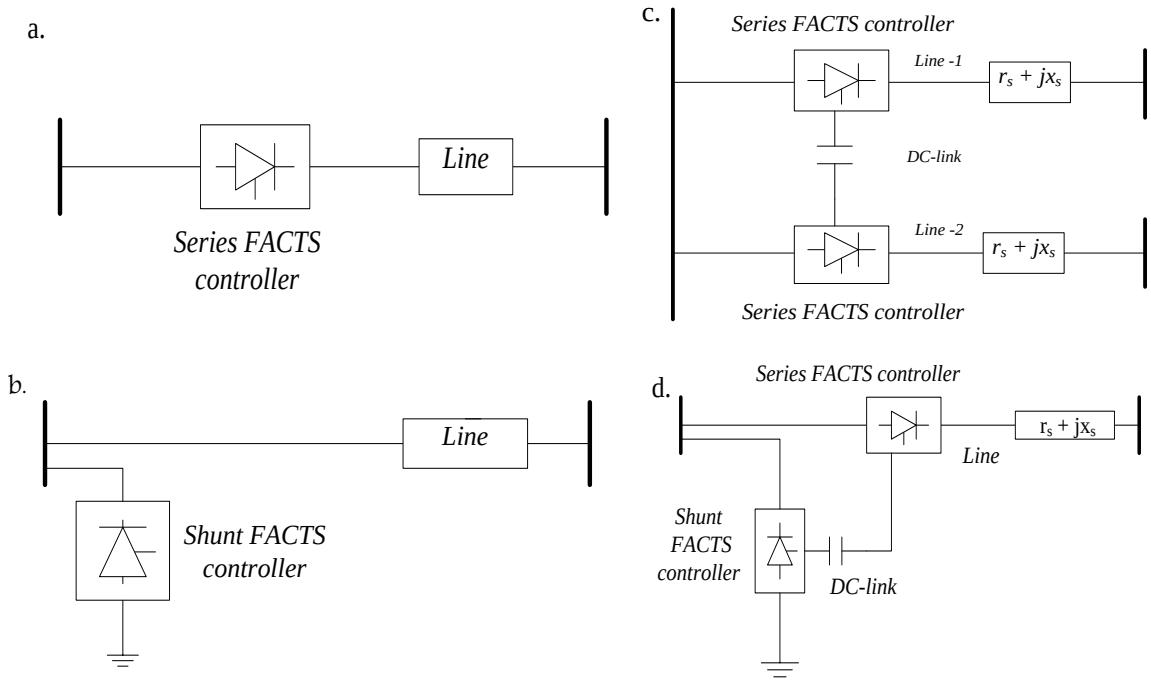

Figure 2.3: FACTS controller's classifications based on their connection in the network, (a) Series controllers, (b) Shunt controllers, (c) Combined series-series controllers, (d) Combined series-shunt controllers.

As shown, FACTS Controllers may be based on thyristor devices with no gate turn off or with power devices with gate turn off capability. Table 2.1 gives an overview of major facts devices in terms of power electronic devices.

The benefit of an added storage system to the controller is significant. A controller with storage is much more effective for controlling the system dynamics than the corresponding controller without the storage. This has to

do with dynamic pumping of real power in or out of the system as against only influencing the transfer of real power within the system as in the case with controllers lacking storage [3].

Table 2.1: Overview of major FACTS devices in terms of power electronic devices

Power electronic devices based	FACTS controllers	Connection in the system
Thyristor Based type	SVC	shunt connected
	TCSC	series connected
	TCPST	combined shunt and series
Voltage Source Converter (VSC) based.	STATCOM	shunt connected
	SSSC	series connected
	IPFC	combined series-series
	UPFC	combined shunt-series

2.5 FACTS devices benefits

FACTS devices enable the transmission owners to obtain one or more of the following benefits:

- Power flow control.
- Increase of transmission capability.
- Voltage control.
- Reactive power compensation, stability improvement.
- Power quality improvement.
- Power conditioning.

Because the voltage, current, impedance, real power, and reactive power are interrelated, each controller has multiple attributes of what they can do in

terms of controlling the voltage, power flow, stability and so on. These controllers can have multiple open loop and closed loop controls to accomplish multiple benefits. Table 2.2 gives a checklist of solutions of steady-state operating problems can be corrected by various controllers [1].

Table 2.2: The role of FACTS controllers in power system operation

Operating problem	Corrective action	FACTS controller
Voltage limits:		
Low voltage at heavy load	Supply reactive power	STATCOM, SVC,
High voltage at low load	Absorb reactive power	STATCOM, SVC, TCR
High voltage following an outage	Absorb reactive power; prevent overload	STATCOM, SVC, TCR
Low voltage following an outage	Supply reactive power; prevent overload	STATCOM, SVC
Thermal limits:		
Transmission circuit overload	Reduce overload	TCSC, SSSC, UPFC, IPC, PS
Tripping of parallel circuits	Limit circuit loading	TCSC, SSSC, UPFC, IPC, PS
Loop flows:		
Parallel line load sharing	Adjust series reactance	IPC, SSSC, UPFC, TCSC, PS
Postfault power flow sharing	Rearrange network or use thermal limit actions	IPC, TCSC, SSSC, UPFC, PS
Power flow direction reversal	Adjust phase angle	IPC, SSSC, UPFC, PS

2.6 Power electronic controllers based on fully controlled semiconductor devices [1]

Converters are used to convert dc power into ac power at desired output voltage and frequency. Modern power system controllers based on power electronic converters are capable of generating reactive power with no need for large reactive energy storage elements, such as in conventional thyristor controlled FACTS controllers. This is achieved by making the currents circulate with the assistance of fast switching devices. The semiconductor devices employed in the new generation of power electronic converters are of the fully controlled type, such as the insulated gate bipolar transistor (IGBT) and the gate turn off thyristor (GTO). Figure 2.4 shows their respective circuit symbols.

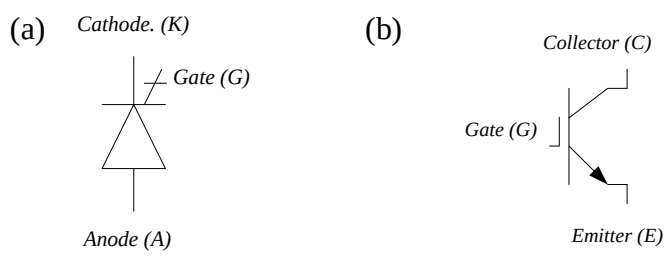

Figure 2.4: Circuit symbols for: (a) gate turn-off thyristor and (b) insulated gate bipolar transistor.

The GTO is a more advanced version of the conventional thyristor, with a similar switched on characteristic but with the ability to switch off at a time different from when the forward current falls naturally below the holding current level. Such added functionality has enabled new application areas in

industry to be developed, but still large negative pulses are required to turn them off.

The IGBT is one of the most well developed members of the family of power transistors. It is the most popular device used in the area of motor drives, reaching power levels of a few hundred kilowatts. Power converters aimed at power systems applications are beginning to make use of IGBTs owing to their increasing power-handling capability and relatively low conduction losses. Further progress is expected in IGBT and GTO technology and applications.

In DC–AC converters that use fully controlled semiconductors rather than conventional thyristors, the DC input can be either a voltage source or a current source with reference to this basic operational principle, converters can be classified as either voltage source converters (VSCs) or current source converters.

For economic and performance reasons, most reactive power controllers are based on the VSC topology. The availability of modern semiconductors with relatively high voltage and current ratings, such as GTOs or IGBTs, has made the concepts of reactive compensation based on switching converters a certainty, even for substantial high-power applications.

A number of power system controllers that use VSCs as their basic building block are in operation in various parts of the world. The most popular are: STATCOMs, SSSCs, the UPFC, and the HVDC-VSC.

2.6.1 Voltage source converter

There are deferent VSC topologies currently in use in actual power system operation and some others that hold great potential, nevertheless there are

common aims of these topologies including minimization of the operating frequency of the semiconductors inside the VSC and producing a high-quality sinusoidal voltage waveform with minimum or no filtering requirements. Figure 2.5 illustrate the topology of a conventional two-level VSC using IGBT switches.

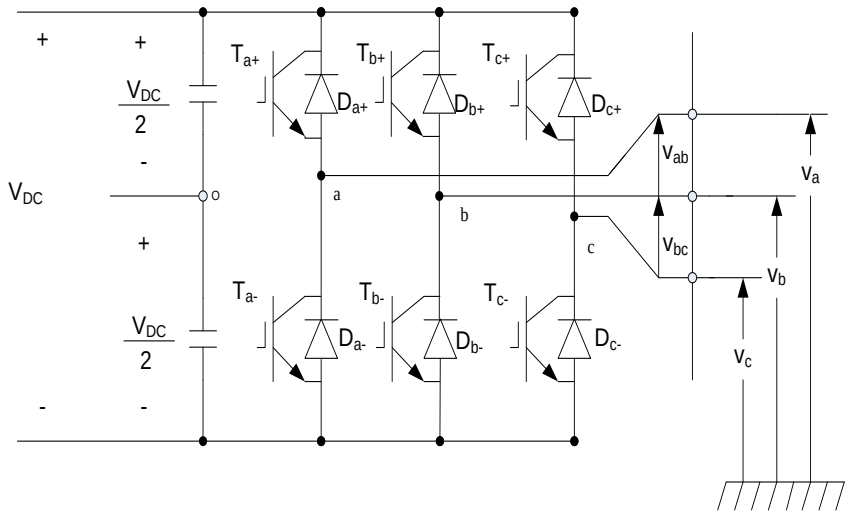

Figure 2.5: Topology of a three-phase, two-level voltage source converter (VSC) using insulated gate bipolar transistors.

The VSC shown in figure 2.5 comprises six IGBTs, with two IGBTs placed on each leg. Moreover, each IGBT is provided with a diode connected anti parallel to make provisions for possible voltage reversals due to external circuit conditions. Two equally sized capacitors are placed on the DC side to provide a source of reactive power. The switching control module is an integral component of the VSC. Its task is to control the switching sequence of the various semiconductor devices in the VSC, aiming at producing an output voltage waveform that is as near to a sinusoidal waveform as possible, with high power controllability and minimum switching loss.

2.6.2 Principles of voltage source converter operation

The interaction between the VSC and the power system may be explained in simple terms, by considering a VSC connected to the AC mains through a lossless reactor, as illustrated in the single-line diagram shown in figure 2.6(a). The premise is that the amplitude and the phase angle of the voltage drop ΔV_x across the reactor X_l, can be controlled, defining the amount and direction of active and reactive power flows through X_l.

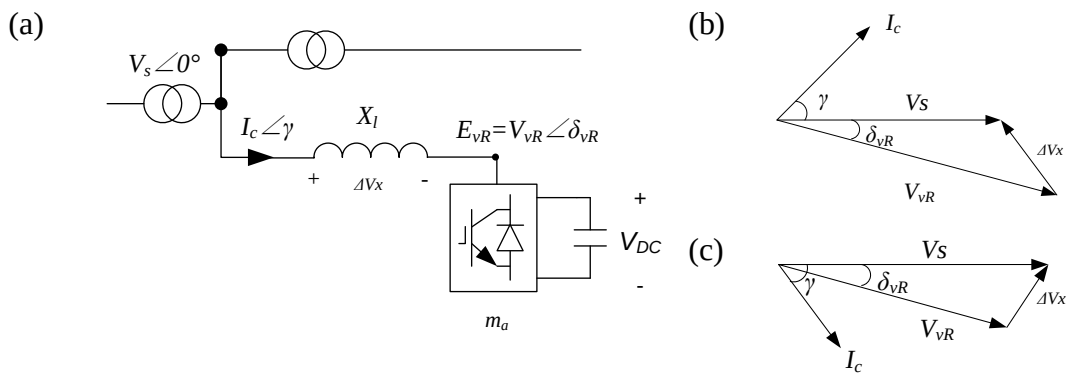

Figure 2.6: Basic operation of a voltage source converter (VSC): (a) VSC connected to a system bus, space vector representation for (b) lagging operation and (c) leading operation.

The voltage at the supply bus is taken to be sinusoidal, of value $V_s\angle 0°$, and the fundamental frequency component of the SVC AC voltage is taken to be $V_{vR}\angle\delta_{vR}$. The positive sequence fundamental frequency vector representation is shown in figures 2.6(b) and 2.6(c) for leading and lagging VAr compensation, respectively.

According to figure 2.6, for both leading and lagging VAr, the active and the reactive powers can be expressed as

$$P = \frac{V_s V_{vR}}{X_l} sin\, \delta_{vR} \tag{2.1}$$

$$Q = \frac{{V_s}^2}{X_l} - \frac{V_s V_{vR}}{X_l} cos\, \delta_{vR} \tag{2.2}$$

Were:

P, Q: are the active and reactive powers of the converter,

V_s *:* is the AC voltage source,

V_{vR}, δ_{vR} : are the VSC output voltage magnitude and angle

X_l : is the VSC series reactor.

With reference to figure 2.6 and the two equations above, the following observations are derived:

- The VSC output voltage V_{vR} lags the AC voltage source V_s by an angle δ_{vR}, and the input current lags the voltage drop across the reactor ΔV_x by π/2.
- The active power flow between the AC source and the VSC is controlled by the phase angle δ_{vR}. Active power flows into the VSC from the AC source for lagging δ_{vR} (δ_{vR} >0) and flows out of the VSC from the AC source for leading δ_{vR} (δ_{vR} <0).
- The reactive power flow is determined mainly by the magnitude of the voltage source V_s, and the VSC output fundamental voltage V_{vR}. For $V_{vR} > V_s$, the VSC generates reactive power and consumes reactive power when V_{vR} < Vs.
- The DC capacitor voltage V_{DC} is controlled by adjusting the active power flow that goes into the VSC. During normal operation, a small amount of active power must flow into the VSC to compensate for the power losses inside the VSC, and δ_{vR} is kept slightly larger than 0°.

The major power system controllers that use the VSC as their basic building block are addressed below with reference to key steady-state operational characteristics and their impact on system voltage and power flow control.

2.6.3 Control capabilities of controllers based on voltage source converters

The employment of the high power controllable output of voltage source converters in FACTS controllers provide them great power control capabilities. They are able to regulate either nodal voltage magnitude or injection of reactive power at one of its terminals, and active power flow through the controller. From the perspective of fundamental frequency power system studies, there is little difference between the control flexibility afforded by these controllers. The individual control functions are illustrated in figure 2.7.

If the VSC is connected to a bus have a voltage magnitude of $V_m\angle\theta_m$, and the injected current at this bus is $I_m\angle\gamma_m$, the bus voltage magnitude can be controlled at a specified value by injecting an in-phase or antiphase voltage increment $\Delta V_{cR}\angle\theta_m$, as illustrated in figure 2.7(a).

Series reactive compensation can be achieved by injecting a complex voltage $\Delta V_{cR}\angle(\gamma_m \pm 90)$ which is in quadrature with the line current $I_m\angle\gamma_m$, as illustrated in figure 2.7(b). Pure phase-angle control is also possible, as shown in figure 2.7(c), by injecting an angular quantity $1\angle\delta_{cR}$, to the otherwise unaffected voltage $V_m\angle\theta_m$. Furthermore, all three functions can be applied simultaneously by injecting an incremental complex voltage $V_{cR}\angle\delta_{cR}$ to $V_m\angle\theta_m$, as shown in figure 2.7(d), a characteristic that adds unrivalled flexibility in power system operation.

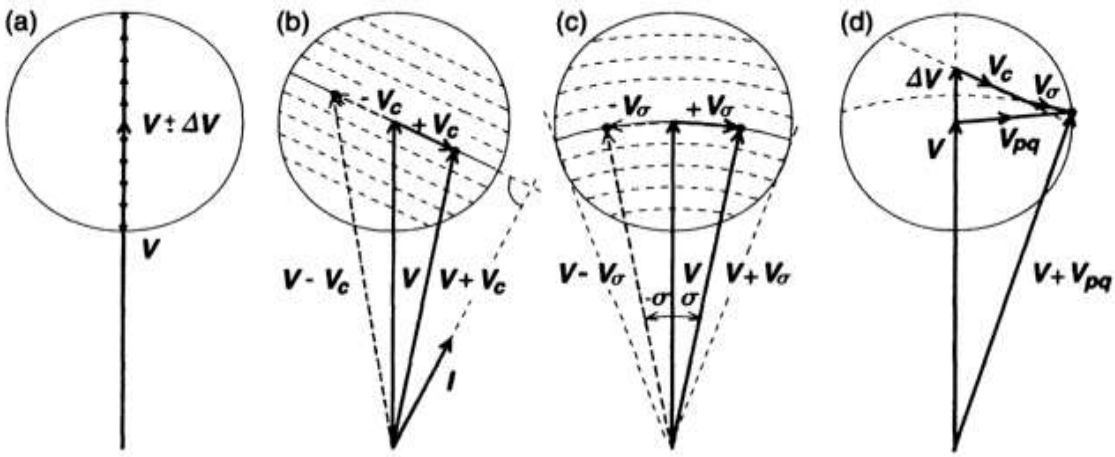

Figure 2.7: Phasor diagram illustrating the general concept of: (a) magnitude voltage control, (b) impedance line compensation, (c) phase-angle regulation, and (d) simultaneous control.

2.7 The unified power flow controller

As shown in the previous sections, UPFC is designed by combining the series compensator (SSSC) and shunt compensator (STATCOM) coupled with a common DC capacitor, it's become clarified that to introduce these two FACTS devices, this section discuss the main component of the UPFC.

2.7.1 The static compensator

The STATCOM consists of one VSC and its associated shunt-connected transformer. It is the static counterpart of the rotating synchronous condenser but it generates or absorbs reactive power at a faster rate because no moving parts are involved. In principle, it performs the same voltage regulation

function as the SVC but in a more robust manner because, unlike the SVC, its operation is not impaired by the presence of low voltages.

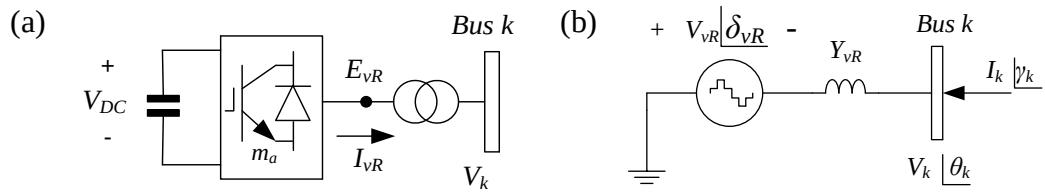

Figure 2.8: Static compensator (STATCOM) system: (a) voltage source converter (VSC) connected to the AC network via a shunt-connected transformer, (b) shunt solid-state voltage source.

A schematic representation of the STATCOM and its equivalent circuit are shown in figures 2.7(a) and 2.7(b), respectively. The equivalent circuit corresponds to the Thevenin equivalent as seen from bus k, with the voltage source E_{vR} being the fundamental frequency component of the VSC output voltage. In steady-state fundamental frequency studies the STATCOM may be represented in the same way as a synchronous condenser, which in most cases is the model of a synchronous generator with zero active power generation. A more flexible model may be realized by representing the STATCOM as a variable voltage source E_{vR}, for which the magnitude and phase angle may be adjusted, using a suitable iterative algorithm, to satisfy a specified voltage magnitude at the point of connection with the AC network. The shunt voltage source of STATCOM may be represented by:

$$E_{vR} = V_{vR}\,(\cos\delta_{vR} + Jsin\,\delta_{vR}) \tag{2.3}$$

The voltage magnitude V_{vR}, is given maximum and minimum limits, which are a function of the STATCOM capacitor rating. However, δ_{vR} may take any value between 0 and 2π radians.

2.7.2 The solid state series compensator

For the purpose of steady-state operation, the SSSC performs a similar function to the static phase shifter; it injects voltage in quadrature with one of the line end voltages in order to regulate active power flow. However, the SSSC is a far more versatile controller than the phase shifter because it does not draw reactive power from the AC system; it has its own reactive power provisions in the form of a DC capacitor. This characteristic makes the SSSC capable of regulating not only active but also reactive power flow or nodal voltage magnitude. A schematic representation of the SSSC and its equivalent circuit are shown in figures 2.8(a) and 2.8(b), respectively.
The series voltage source of SSSC may be represented by

$$E_{cR} = V_{cR} (\cos \delta_{cR} + Jsin\ \delta_{cR}) \qquad (2.4)$$

The magnitude and phase angle of the SSSC model are adjusted by using any suitable iterative algorithm to satisfy a specified active and reactive power flow across the SSSC.
Similar to the STATCOM, maximum and minimum limits will exist for the voltage magnitude V_{cR}, which are a function of the SSSC capacitor rating; the voltage phase angle δ_{cR} can take any value between 0 and 2π radians.

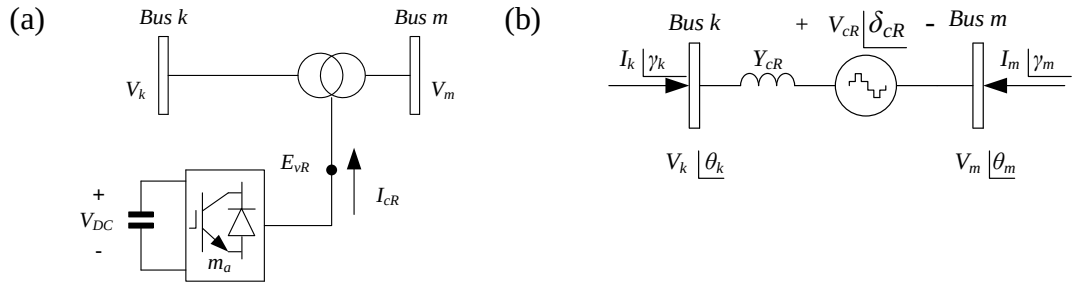

Figure 2.9: Solid state series compensator (SSSC) system: (a) voltage source converter (VSC) connected to the AC network using a series transformer and (b) series solid state voltage source.

UPFC is introduced by combining the two FACTS devices STATCOM and SSSC. The UPFC may be seen to consist of two VSCs sharing a common capacitor on their DC side and a unified control system. A simplified schematic representation of the UPFC is given in figure 2.9(a), together with its equivalent circuit, in figure 2.9(b)

The UPFC allows simultaneous control of active power flow, reactive power flow, and voltage magnitude at the UPFC terminals. Alternatively, the controller may be set to control one or more of these parameters in any combination or to control none of them.

The active power demanded by the series converter is drawn by the shunt converter from the AC network and supplied to bus m through the DC link; this way allows the voltage across the capacitor constant [19]. The output voltage of the series converter is added to the nodal voltage, at say bus k, to boost the nodal voltage at bus m. The voltage magnitude of the output voltage V_{cR} provides voltage regulation, and the phase angle δ_{cR} determines the mode of power flow control.

(a)

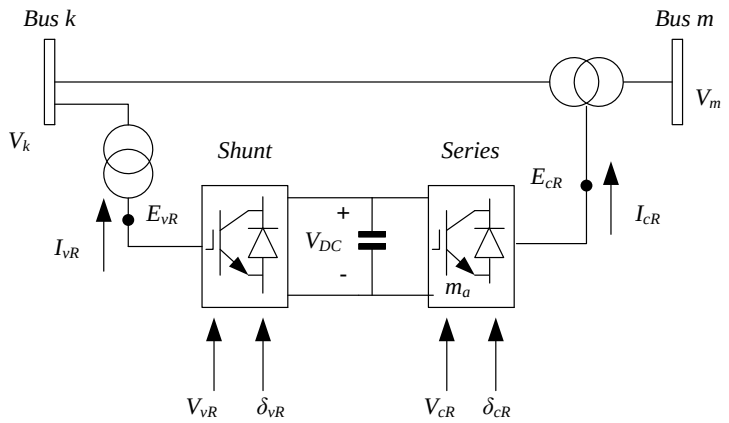

(b)

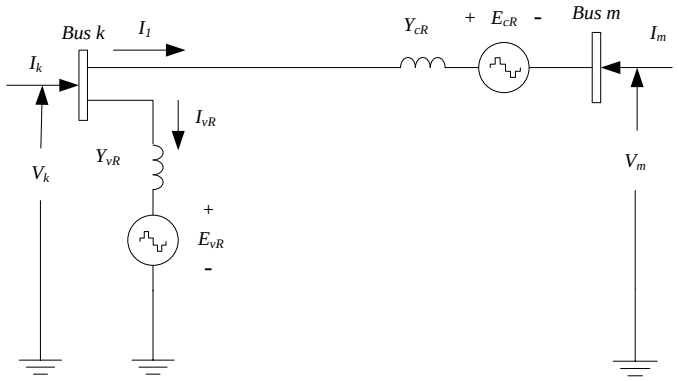

Figure 2.10: Unified power flow controller (UPFC) system: (a) two back-to-back voltage source converters (VSCs), (b) equivalent circuit based on solid-state voltage sources.

In addition to provide a supporting role in the active power exchange that takes place between the series converter and the AC system, the shunt converter may also generate or absorb reactive power in order to provide independent voltage magnitude regulation at its point of connection with the AC system [1].

The UPFC equivalent circuit shown in figure 2.9(b) consists of a shunt connected voltage source, a series connected voltage source, and an active power constraint equation, which links the two voltage sources. The two voltage sources are connected to the AC system through inductive reactance

representing the VSC transformers. Suitable expressions for the two voltage sources and constraint equations would be:

$$E_{vR} = V_{vR}\,(cos\,\delta_{vR} + Jsin\,\delta_{vR}), \tag{2.5}$$

$$E_{cR} = V_{cR}\,(cos\,\delta_{cR} + Jsin\,\delta_{cR}), \tag{2.6}$$

$$Re\{E_{vR}\,I_{vR}^{*} + E_{cR}\,I_{m}^{*}\} = 0. \tag{2.7}$$

2.7.3 Basic principle of UPFC operation

It follows from that discussion that an equivalent circuit consisting of two coordinated synchronous voltage sources should represent the UPFC adequately for the purpose of fundamental frequency steady-state analysis. Such an equivalent circuit is shown in figure 2.10. The synchronous voltage sources represent the fundamental voltage waveforms at the AC converter terminals of the UPFC.

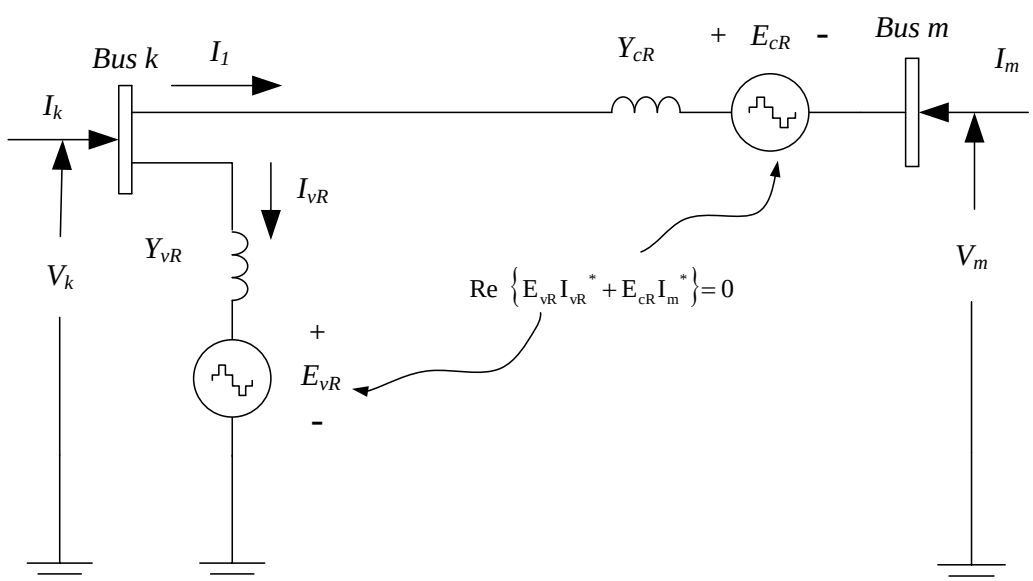

Figure 2.11: Unified power flow controller equivalent circuit.

The UPFC voltage sources are:

$$E_{vR} = V_{vR}\,(\cos\delta_{vR} + Jsin\,\delta_{vR}),$$
$$E_{cR} = V_{cR}\,(\cos\delta_{cR} + Jsin\,\delta_{cR}),$$

Where V_{vR} and δ_{vR} are the controllable magnitude and phase angle of the voltage source representing the shunt converter.

$$(V_{vR\,\min} \leq V_{vR} \leq V_{vR\,\max})$$
$$(0 \leq \delta_{vR} \leq 2\pi)$$

The magnitude V_{cR} and phase angle δ_{cR} of the voltage source representing the series converter are controlled between limits

$$(V_{cR\,\min} \leq V_{cR} \leq V_{cR\,\max})$$
$$(0 \leq \delta_{cR} \leq 2\pi).$$

The phase angle of the series injected voltage determines the mode of power flow control. If δ_{cR} is in phase with the nodal voltage angle θ_k, the UPFC regulates the terminal voltage. If δ_{cR} is in quadrature with respect to θ_k, it controls active power flow, acting as a phase shifter. If δ_{cR} is in quadrature with the line current angle, then it controls active power flow acting as a variable series compensator. At any other value of δ_{cR}, the UPFC operates as a combination of voltage regulator, variable series compensator, and phase shifter. The magnitude of the series injected voltage determines the amount of power flow to be controlled [7].

Based on the equivalent circuit presented in figure 2.10, the two power injection in busses and for load flow analysis can be calculated according to the following expressions in (2.8)–(2.14) [1], [18]:

Series converter:

$$P_{cR} = V_{cR}^2\, G_{mm} + V_{cR}\, V_k [\, G_{km} \cos(\delta_{cR} - \theta_k) + B_{km} sin(\delta_{cR} - \theta_k)] \quad (2.8)$$
$$+ V_{cR}\, V_m [\, G_{mm} \cos(\delta_{cR} - \theta_m) + B_{mm} sin(\delta_{cR} - \theta_m)]$$
$$Q_{cR} = -V_{cR}^2\, B_{mm} + V_{cR}\, V_k [\, G_{km} \sin(\delta_{cR} - \theta_k) - B_{km} cos(\delta_{cR} - \theta_k)] \quad (2.9)$$
$$+ V_{cR}\, V_m [\, G_{mm} \sin(\delta_{cR} - \theta_m) + B_{mm} cos(\delta_{cR} - \theta_m)]$$

Shunt converter:

$$P_{vR} = -V_{vR}^2\, G_{vR} + V_{vR}\, V_k [\, G_{vR} \cos(\delta_{vR} - \theta_k) + B_{vR} sin(\delta_{vR} - \theta_k)] \quad (2.10)$$
$$Q_{vR} = V_{vR}^2\, B_{vR} + V_{vR}\, V_k [\, G_{vR} \sin(\delta_{vR} - \theta_k) - B_{vR} cos(\delta_{vR} - \theta_k)] \quad (2.11)$$

Assuming loss-less converter valves, the active power supplied to the shunt converter, P_{vR} equals the active power demanded by the series converter, P_{cR}; that is,

$$P_{vR} + P_{cR} = 0 \quad (2.12)$$

Accordingly, apparent power exchanged through series injected voltage:

$$S_{cR} = P_{cR} + j\, Q_{cR} = E_{cR}\, I_m{}^* \quad (2.13)$$

($P_{cR} > 0$, $Q_{cR} > 0$) implies that active and reactive power is injected into the system.

Apparent power exchanged through shunt current:

$$S_{vR} = P_{vR} + j\, Q_{vR} = E_{vR}\, I_{vR}{}^* \quad (2.14)$$

($P_{vR} > 0$, $Q_{vR} > 0$) implies that active and reactive power is drawn from the system. The reactive powers Q_{cR} and Q_{vR}, however, can be independently produced by the two converters.

The fast switching capability of the VSCs enables the UPFC to provide fast dynamic response if properly designed. Even though the shunt–series type topology is ideal for power flow control, the VSC-based UPFC has two major drawbacks: its high installation and operating costs. Moreover, the fast dynamic response in the range of ms is not required in most utility applications. Traditionally, a mechanical LTC is used since its speed of operation provides adequate response time in most utility applications. If faster response is needed, the mechanical LTCs can be replaced with faster switches [6].

CHAPTER THREE

PLACEMENT STRATEGY OF UPFC

3.1 Introduction

This chapter discusses the methodology approach in simulating the Sudanese national electrical system using proper software. The main objective of this project is to improve voltage profile and reduce transmission power losses by incorporating UPFC to the system.

Sudanese national electrical system is used as a model. The impact of UPFC on Sudanese national electrical system is important for this study. Therefore, studying the analyses and the impacts of incorporate FACTS controllers to electrical system is significant to access to the problem formulation. The simulation is run by using NEPLAN and MATPOWER software.

3.2 Optimal location for UPFC

Distribution networks experience distinct change from a low to high load level every day. Hence, a major concern in power distribution networks is the problem of voltage stability [15]. A formula for calculating the voltage stability index (VSI) can be generated to calculate the VSI in every line in the system and then identify the candidate location for FACTS devices. Power flow study must be done in order to determine the steady-state operation of the electric power system. It calculates the voltage drop on each

feeder, the voltage at each bus, and the power flow in all branch and feeder circuits.

There are many indices which use the elements of the admittance matrix and some system variables such as bus voltages and power flow through lines such as VCPI [10], L-index [11], L_{mn} [12], LQP [13] and FVSI [14]. Some of these indices use the concept of the maximum power transfer that can be transmitted to the load bus in a simple two bus power system. These indices require less computational effort and are suitable for quickly diagnosing the power system voltage stability.

The L_{mn} have a better response when the increased is just from reactive power flow is higher than the active power flow. Due to high reactive power flow in Sudanese electrical network L_{mn} is used to identify the weakest line in the network.

3.2.1 Line Stability Index (L_{mn}) calculation

Most of line stability indices are formulated based on the power transmission concept in a single line. A single line in an interconnected network is illustrated in Figure 3.1.

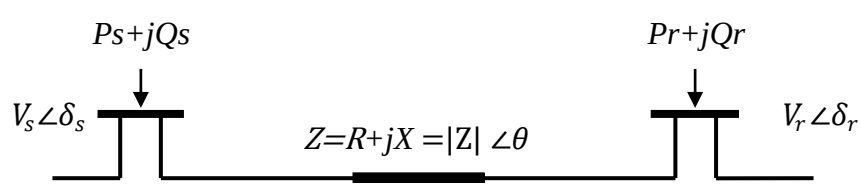

Figure 3.1: Two bus system.

Where,

Vs, Vr: are the sending end and receiving end voltages.

$\delta s, \delta r$: are the phase angles at the sending and receiving end.

Z: is the line impedance.

R: is the line resistance.

X: is the line reactance.

θ: is the line impedance angle.

Ps, Qs: are the active and reactive powers at the sending end.

Pr, Qr: are the active and reactive powers at the receiving end.

This index proposed in [16] is based on the concept of power flow through a single line and adopting the technique of reducing a power system network into a single line.

The line current I_{line}, is calculated by:

$$I_{line} = \frac{(Vs - Vr)}{Z} \tag{3.1}$$

The I_{line} also can be determined by using the receiving apparent power given as:

$$I_{line} = \left(\frac{S_r}{V_r}\right)^* = \left(\frac{P_r - jQ_r}{V_r \angle -\delta_r}\right) \tag{3.2}$$

Rearranging equation (3.1) and (3.2) yields:

$$P_r - jQ_r = \frac{|Vs||Vr|}{Z}\angle(\theta - \delta s + \delta r) - \frac{|Vr|^2}{Z}\angle\theta \tag{3.3}$$

If this equation is separated in real and reactive power, then,

$$P_r = \frac{|Vs||Vr|}{Z} cos(\theta - \delta s + \delta r) - \frac{|Vr|^2}{Z} cos\theta \tag{3.4}$$

$$Q_r = \frac{|Vs||Vr|}{Z} sin(\theta - \delta s + \delta r) - \frac{|Vr|^2}{Z} sin\theta \tag{3.5}$$

Defining $\delta = \delta s - \delta r$ and solving equation 3.5 for Vr, then,

$$V_r = \frac{V_s\, sin(\theta - \delta) \pm \sqrt{\left(V_s\, sin(\theta - \delta)\right)^2 - (4XQ_r)}}{2\sin(\theta)} \tag{3.6}$$

If we substitute $Z\, sin\theta = X$ and consider the condition that the value of the square root must be positive,

$$\begin{cases} \left(V_s\, sin(\theta - \delta)\right)^2 - (4XQ_r) \geq 0 \\ L_{mn} = \dfrac{4XQ_r}{\left(V_s\, sin(\theta - \delta)\right)^2} \leq 1 \end{cases} \tag{3.7}$$

This VSI is used to find the stability index for each line connection between two bus bars in an interconnected network. As long as L_{mn} remains less than one the system is stable, once the value of L_{mn} exceeds one, the system reaches its voltage collapse point.

In voltage collapse studies, the continuation method shows many advantages, so, most of the researchers apply this technique to trace voltage profile at various busses of the test power system, with respect to changes of loading level λ , namely, Continuation Power Flow (CPF).

To demonstrate the effectiveness of the proposed index, each generated and loaded power is increased gradually until one of L_{mn} values reach its unstable point, then the system reaches to the stability margin. The variation of load in the entire load busses changes the value of L_{mn} . The best L_{mn} values are selected at the maximum loading point.

3.3 UPFC parameter setting

Optimal power flow (OPF) solution methods have been developed over the years to meet the practical requirement of power system operation, The OPF solution includes an objective function that is optimized without violating the system operating constraints. These include the network equations, loading conditions, and physical limits on active and reactive power generation.

In this thesis OPF is performed to determine the optimal steady-state operating conditions of the power network, voltage magnitudes and angles at all busses of the network, and optimal active and reactive power flow in transmission lines. The selected objective function for OPF is to minimize the active power losses in the network. OPF is done using NEPLAN software.

OPF results at the suggested optimal locations are used to adjust the power flow parameters setting for the UPFC's, which are the control value of the active line flow, control value of the reactive line flow, and control value of the voltage magnitude at the sending bus.

Different equations exist for the purpose of determining the working ranges for UPFC parameters, these equations (2.8 - 2.14) are discussed at the previous chapter.

If the range of these parameters does not specified correctly, UPFC failed to control the active and reactive power flow at the selected values, consequently the power flow program will not converges to the solution.

Depending on the operating condition exhibited by the OPF, controlled active and reactive power at the candidate locations are specified, and

V_{cR}, I_q ranges is adapted to enable the UPFC's to accomplish the required power flow profile, accordingly for all UPFC devices will be installed in this thesis the following identifications have been made :

(a) The source impedances of UPFC's have been neglected.

(b) Working range for the series voltage source magnitude V_{cR} is [0, 0.3] p.u.

(c) Working range for the shunt reactive current I_q is [0, 190] A.

(d) Maximum power through the DC link is 50 MW.

3.4 Criteria for optimal location of UPFC

The following criteria have been used for optimal placement of UPFC.

- The branches having transformers have not been considered for the UPFC placement.
- The line having the highest value of L_{mn} is considered the best location for UPFC, followed by other lines having less value.
- When two or more cascaded lines in a radial network are considered as the best location, then the line having the highest value of L_{mn} of this radial network is considered as the best location for UPFC placement.
- The UPFC's is installed one by one and the system improvements are compared with the previous case until there are no improvement considered.

The flowchart of the proposed approach to find the appropriate locations in power system network for UPFC placement is presented in figure 3.2.

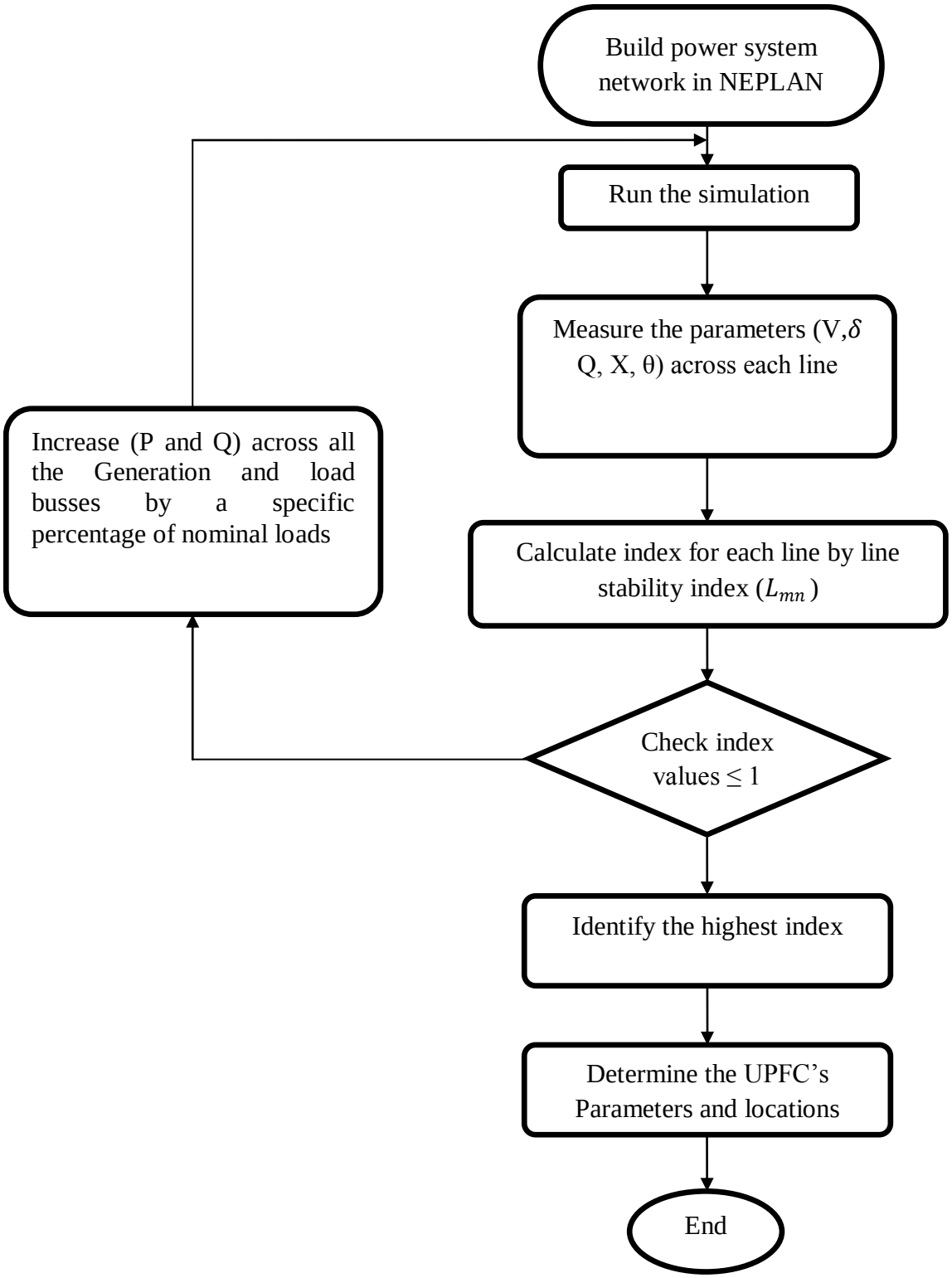

Figure 3.2: Flow chart of the proposed approach.

3.5 Software developments

To simplify the study, commercial software NEPLAN has been implemented to introduce UPFC's in the system and to obtain the power flow results. NEPLAN is one of the most complete planning, optimization and simulation tool for transmission, distribution, generation and industrial networks [24]. It is used in more than 80 countries by more than 600 companies, such as small and large electrical utilities, industries and universities [25].

NEPLAN includes power flow, optimal power flow, reliability, protection systems, harmonic analysis, transient stability, power quality and models of various FACTS devices. All operations can be assessed by means of graphical user interfaces (GUIs).

The connection of UPFC in NEPLAN is shown in figure 3.3, and the main UPFC parameters needed is shown in table 3.1.

3.5.1 Description of UPFC in NEPLAN

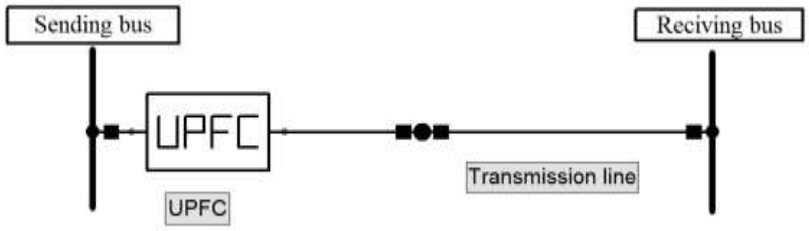

Figure 3.3: Schematic symbol of UPFC in NEPLAN.

Table 3.1: UPFC Parameters

Name	**Name of element.**
V_{cR} min	Minimum series voltage magnitude in % of the bus nominal voltage.
V_{cR} max	Maximum series voltage magnitude in % of the bus nominal voltage.
I_q min	Minimum shunt current in A.
I_q max	Maximum shunt current in A.
Pmax	Maximum power through the DC link (Px) in MW.
P	Control value for the active line flow P2.
Q	Control value for the reactive line flow Q2.
Sending end V set	Control value for the voltage magnitude of the sending end.
Receiving end V min	Minimum voltage magnitude at the receiving end.
Receiving end V max	Maximum voltage magnitude at the receiving end.

MATPOWER is a package of MATLAB M-files; it is provide a function for continuation power flow. Sudanese electrical network is converted to MATPOWER format in order to utilize this function as shown in appendix A to carry out the line stability index which proposed in section 3.2.1.

Sudanese electrical network is discussed in the next chapter, and then the results of the placement technique are shown, also the improvement in voltage profile and transmission power losses reduction is discussed.

CHAPTER FOUR

SIMULATION AND RESULTS

4.1 Sudanese electrical network

The real network of Sudanese electrical power grid was chosen as a test power network. This regional network can be assumed as the typical for the whole country's network in terms of its design and existing problems. The simplified single line diagram of the network is given at figure 4.1. The network has the following characteristics:

Number of busses	82
Number of lines	81
Power plants	8
Loads	53
Shunts	10
Transformers	15

This network include four voltage levels: a 500, 220, 110 and 66 kV which forms the main part of the transmission system in the Sudanese electrical network, the power generated in Sudan comes from seven power plants, Merowe which represent the slack bus bar, Garri, Roseires, Khartoum North, Rabak, Sennar , and Girba, and one tie line feeder from Ethiopia.

Transmission line charge supplies the network by a proper amount of reactive power due to the long length of lines which totaling 5469.735 km long.

This data is taken at normal load condition, the total loading level of the system is 1553.3 MW and 1083.3 MVAr, and the total power generated is 1603.517 MW, 227.008 MVAr. Network data is shown at appendix B.

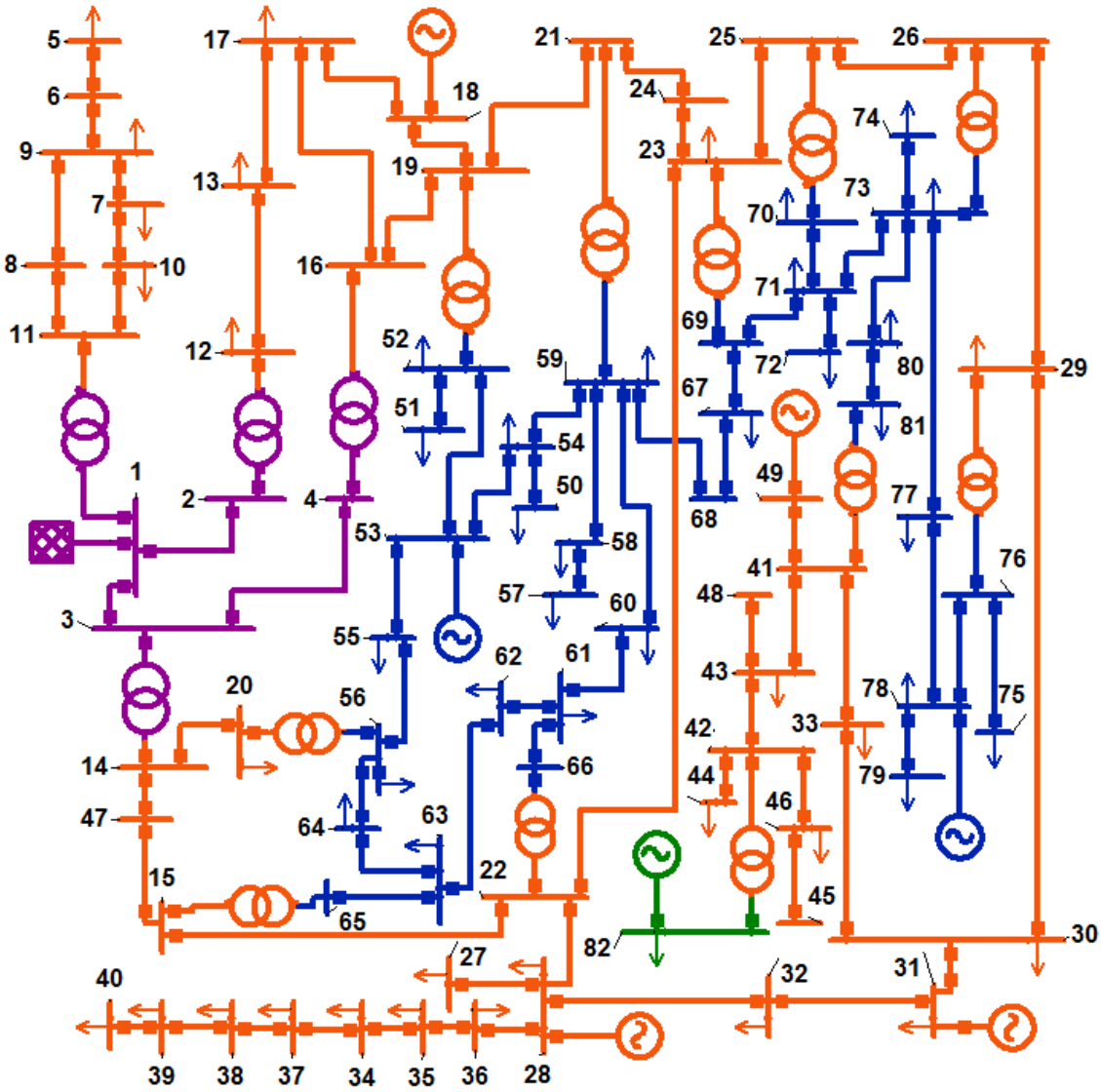

● 500 kV, ● 220 kV, ● 110 kV, ● 66kV

Figure 4.1: Single line diagram of Sudanese electrical network.

Table 4.1 shows the bus voltages and angles at base case and table 4.2 shows the load flow result at base case.

Table 4.1: Bus voltage and angle at base case

Bus number	Bus name	Per Unit Voltage	Voltage kV	Angle Degree
1	MWP500	1	500	0
2	ATB5	1.0031	501.571	-3.7
3	MRK5	0.9777	488.86	-7.6
4	KAB5	0.9799	489.951	-8.3
5	WHL2	0.9892	217.619	-8.7
6	WWA2	1.0204	224.494	-8
7	DEB2-B1	1.0216	224.748	-6.2
8	DEB2-B2	1.0443	229.741	-5
9	DON2	1.0256	225.643	-7.7
10	MWT2	1.0315	226.925	-2.8
11	MWP2	1.0384	228.452	-1.5
12	ATB2	0.924	203.269	-9.1
13	SHN2	0.9688	213.146	-13.8
14	MRK2	1.0051	221.126	-19.4
15	GAM2	0.9844	216.561	-20.4
16	KAB2	0.9871	217.166	-16.6
17	FRZ2	0.9976	219.471	-16.4
18	GER2	1	220	-16.4
19	IBA2	0.9951	218.929	-18.6
20	MHD2	1.0045	220.998	-20
21	KLX2	0.9938	218.637	-19.4
22	JAS2	0.9812	215.854	-20.8
23	GAD2	0.9831	216.286	-21
24	SOB2	0.9914	218.117	-19.8
25	NHAS2	0.9574	210.632	-23.5
26	MAR2	0.9559	210.298	-24.2
27	MSH2	0.996	219.127	-20.6
28	RBK2	1	220	-20.1
29	SNJ2	0.971	213.631	-23.7
30	SNG2	0.9893	217.655	-23.1
31	ROS2	1	220	-18.5
32	RNK2	1.0079	221.742	-19.4
33	HWT2	0.9983	219.626	-23.7
34	OBD2	0.9987	219.71	-23.2
35	UMR2	1.0054	221.199	-21.6
36	TND2	1.0072	221.586	-21.1
37	DBT2	1.0019	220.411	-23.9
38	ZBD2	1.0006	220.142	-24.1
39	FUL2	1.0026	220.571	-24.6
40	BBN2	1.0046	221.01	-24.7
41	GDF2	0.9983	219.615	-24.2

42	GRB2	0.9916	218.151	-24.6
43	SHK2	0.9978	219.523	-24.2
44	NHLF2	0.9914	218.106	-24.7
45	ARO2	0.9982	219.615	-25
46	KSL2	0.9972	219.382	-25
47	HUD	1.0002	220.04	-19.6
48	UTP2	0.9983	219.618	-24.2
49	SHD2	1	220	-23
50	KHE1	0.9821	108.036	-26.8
51	IZB1	0.9663	106.289	-25.7
52	IBA1	0.9734	107.077	-25.3
53	KHN1	1	110	-26.4
54	KUK1	0.9848	108.328	-26.6
55	IZG1	0.975	107.248	-26.3
56	MHD1	0.9642	106.058	-25.9
57	FAR1	0.9288	102.171	-26.8
58	AFR1	0.9364	103.006	-26.4
59	KLX1	0.944	103.836	-26
60	LOM1	0.9441	103.849	-26.2
61	SHG1	0.9516	104.681	-26.3
62	MUG`	0.9547	105.018	-26.5
63	BNT1	0.9585	105.43	-26.4
64	OMD1	0.9576	105.331	-26.4
65	GAM1	0.9858	108.442	-25.5
66	JAS1	1.0035	110.382	-24.7
67	BAG1	0.9203	101.232	-24
68	SOB1 B2	0.9355	102.902	-25.3
69	GAD B2	0.924	101.635	-23.6
70	NHAS1	1.0349	113.836	-25.7
71	OHAS1	1.0317	113.489	-25.9
72	GND1	1.0284	113.124	-26.1
73	MAR1 B1	1.0291	113.2	-26.8
74	MAN1	1.0186	112.047	-27.6
75	ORBK1	1.0197	112.17	-25.2
76	SNJ 1	1.0201	112.214	-25.1
77	HAG1	1.0116	111.274	-26.3
78	SNP1	1	110	-24.8
79	MIN1	0.9481	104.292	-25.8
80	FAO1	1.0049	110.54	-27.2
81	GDF 1	1.0165	111.82	-25.5
82	GRB6	1	66	-25.5

denotes the busses near to the voltage limits.

Table 4.2: Power flow results at base case

From bus	To bus	Line	P MW	Q MVAr	Loading %	P Loss MW	Q Loss MVAr
69	67	1	44.524	-4.279	29.89	0.2022	0.1612
6	5	2	14.547	0.568	3	0.1867	-40.2693
7	9	3	21.267	-17.281	8.28	0.106	-19.4675
11	10	4	85.533	7.309	25.52	0.373	-3.0979
12	13	5	143.335	-143.447	23.04	3.9588	-31.9876
11	8	6	44.682	-24.022	15.08	0.537	-23.0091
10	7	7	55.352	-10.089	16.84	0.629	-16.7687
9	6	8	14.577	-26.665	3.11	0.0302	-68.8835
8	9	9	44.145	-1.013	13.06	0.4089	-18.3098
1	2	10	246.304	-150.523	11.53	1.6304	-227.912
1	3	11	684.998	-263.563	15.16	9.2555	-604.129
3	4	12	277.801	-97.047	12.03	0.3596	-32.6829
13	17	13	106.113	-132.075	18.36	1.9928	-36.1638
17	18	14	33.929	-182.002	19.48	0.1179	-1.5076
16	19	15	333.782	-157.923	39.27	2.8673	1.2191
52	51	16	68.208	39.774	17.03	0.2017	-0.2175
52	53	17	84.91	-214.318	49.72	1.8548	6.2865
54	50	18	82.004	53.171	41.67	0.0874	0.0436
56	55	19	36.399	-126.481	28.66	0.4105	0.9014
53	54	20	119.754	255.433	61.7	0.5689	4.1539
53	55	21	39.302	177.206	38.11	1.1016	3.2608
14	20	22	192.848	-41.056	20.59	0.5546	-6.1948
58	57	23	50.427	32.694	13.47	0.1614	-0.561
59	58	24	67.847	41.074	17.64	0.2164	-0.0968
59	54	25	9.157	-170.897	61	1.7158	6.4934
59	60	26	88.699	-25.444	20.52	0.0793	0.0529
60	61	27	3.276	-83.515	18.59	0.1679	-0.0219
61	62	28	22.242	-29.819	8.21	0.0456	-0.8095
63	62	29	53.361	71.598	19.56	0.0916	0.0225
56	64	30	82.377	40.839	20.02	0.2351	0.095
64	63	31	0.83	-13.686	3.01	0.0032	-0.5247
65	63	32	112.875	118.907	34.92	1.2724	3.5599
21	24	33	153.925	26.495	24.26	0.1945	-1.6716
24	23	34	153.73	28.167	24.33	0.651	-5.3725
67	68	35	7.832	-28.676	59.07	0.5314	0.1362
68	59	36	7.3	-28.812	58.11	0.2876	0.0593
66	61	37	85.901	97.463	27.18	1.851	3.7283
22	23	38	22.764	-31.731	4.18	0.0294	-13.6741
23	25	39	127	37.85	20.81	1.2962	-15.3411
71	69	40	12.22	30.333	57.97	2.3977	0.4865
70	71	41	57.355	44.239	14.69	0.0681	-0.2566

71	72	42	27.859	12.823	6.24	0.0375	-1.4297
71	73	43	6.12	-4.525	13.49	0.0746	-1.8188
27	22	44	18.415	2.438	1.96	0.1374	-56.7841
28	27	45	25.455	-14.229	3.06	0.0518	-42.201
25	26	46	43.619	-8.553	7.17	0.0898	-13.3328
73	74	47	10.955	1.737	11.31	0.069	-2.321
29	26	48	27.807	26.037	6.06	0.1493	-20.6009
73	77	49	2.861	11.857	21.68	0.1554	-1.0033
78	77	50	5.091	-10.562	21.44	0.2031	-1.7386
76	78	51	18.419	43.677	84.98	0.6251	0.4227
76	75	52	0.336	-1.788	3.26	0.0004	-3.2643
78	79	53	14.999	8.157	31.22	0.6175	-1.3946
73	80	54	6.699	3.315	13.28	0.1263	-2.2482
30	29	55	63.414	68.531	14.57	0.3883	-11.1206
31	30	56	106.99	-25.893	16.99	1.6	-39.8294
31	32	57	32.677	-55.995	6.81	0.1805	-55.3223
30	33	58	29.946	-60.179	7.13	0.173	-34.6115
28	36	59	44.81	-56.136	7.54	0.2436	-43.4277
35	34	60	39.827	-12.3	8.7	0.2737	-24.026
34	37	61	19.797	-20.052	5.92	0.064	-17.4264
37	38	62	13.483	-6.564	3.14	0.0165	-13.0728
38	39	63	10.106	-17.255	4.2	0.0216	-23.6209
39	40	64	3.364	-13.28	2.87	0.0044	-15.7832
36	35	65	43.558	-18.268	4.92	0.1017	-31.0856
32	28	66	32.094	-23.057	4.12	0.1251	-64.7524
33	41	67	28.227	-26.525	4.07	0.0585	-39.346
42	46	68	16.729	-43.68	4.95	0.0609	-37.0655
43	42	69	42.126	7.796	4.51	0.1091	-27.0712
41	43	70	42.81	6.018	4.55	0.0108	-3.2184
46	45	71	0.002	-17.292	1.82	0.0023	-17.2922
42	44	72	12.034	-11.04	1.73	0.0051	-19.0608
14	47	73	205.094	145.822	26.28	0.3937	-2.0127
47	15	74	204.7	147.835	26.5	1.2676	-5.8611
17	16	75	56.616	77.43	10.09	0.2754	-13.7576
43	48	76	0.001	-11.075	1.17	0.0006	-11.0751
18	19	77	219.811	-33.218	23.34	2.0254	-15.5831
19	21	78	354.255	-54.382	37.81	1.2541	-0.4641
49	41	79	38	-44.326	6.13	0.1984	-76.1212
81	80	80	4.547	-4.236	8.67	0.0982	-5.2118
15	22	81	90.557	11.059	9.73	0.1694	-9.9772
Total						**50.1895**	**-1943.18**

denotes the lines loaded above 50% of its rating.

Sudanese national electrical company applies ±10% of the nominal voltage as acceptable statutory voltage limits. At the base case all busses are within the allowable limit, however six busses in the network are near to the lower statutory limit. Figure 4.2 shows these weak busses and figure 4.3 shows the voltage profile for all busses.

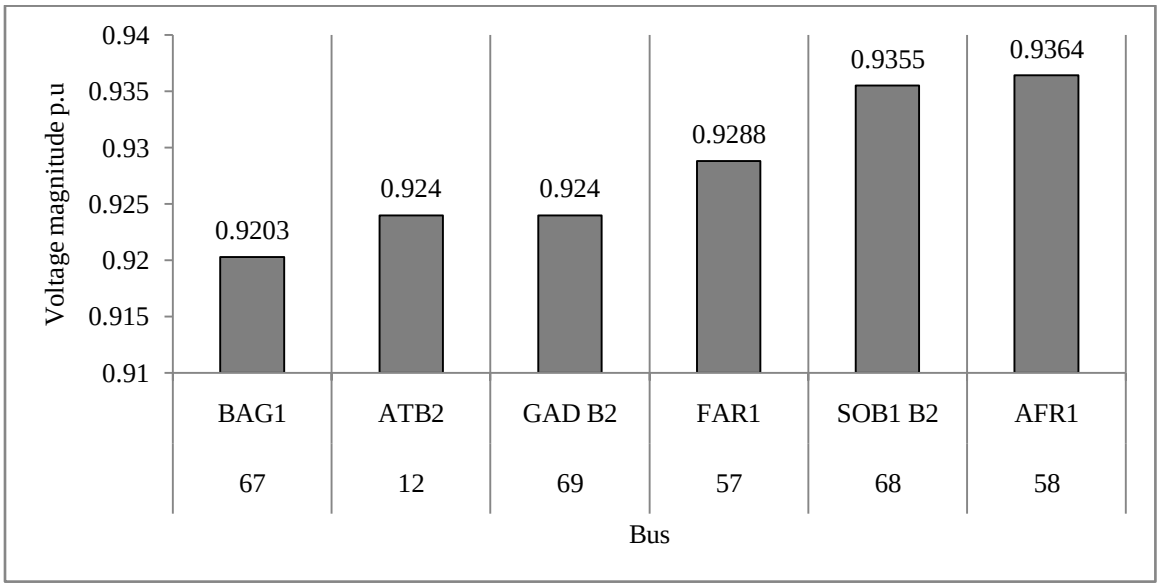

Figure 4.2: Busses near to the lower limit.

Total active and reactive power losses are found to be 50.1895MW and -1943.18 MVAr respectively. The lines near the slack bus have the highest active and reactive power flow. Line 11 (MWP500 - MRK5) shows 9.2555MW and -604.129MVAr active and reactive power loss respectively, which represent the highest active and reactive power loss in the network.

Although this data is taken at normal loading conditions there are six lines loaded above 50% of its maximum loading rate. Figures (4.4 - 4.8) shows the power flow and losses in the transmission lines and its percentage loading.

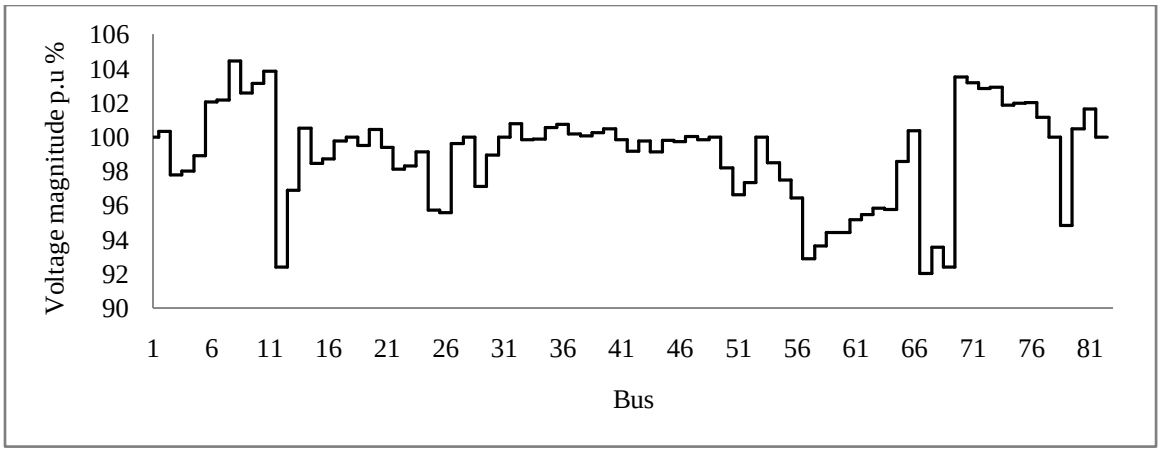

Figure 4.3: Voltage profiles at base case.

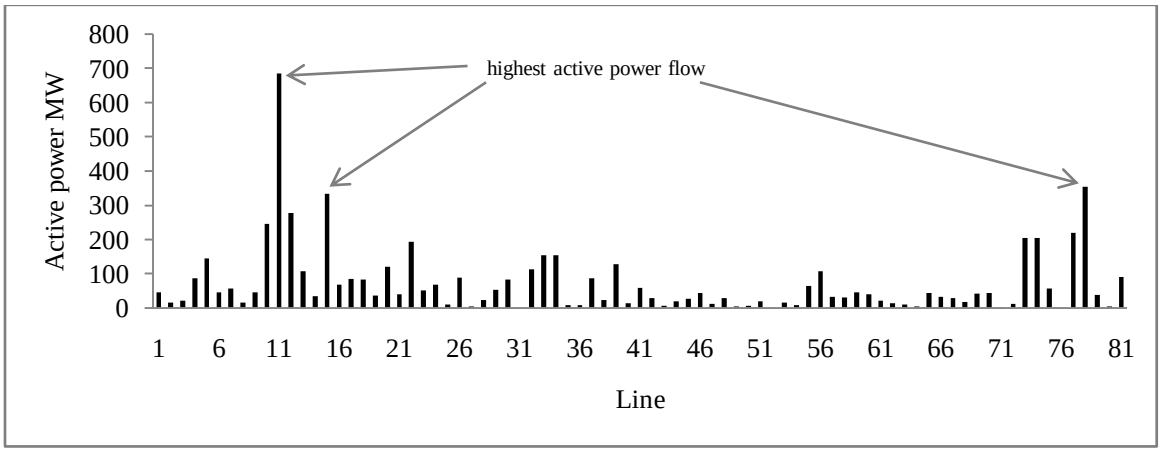

Figure 4.4: Active power at base case.

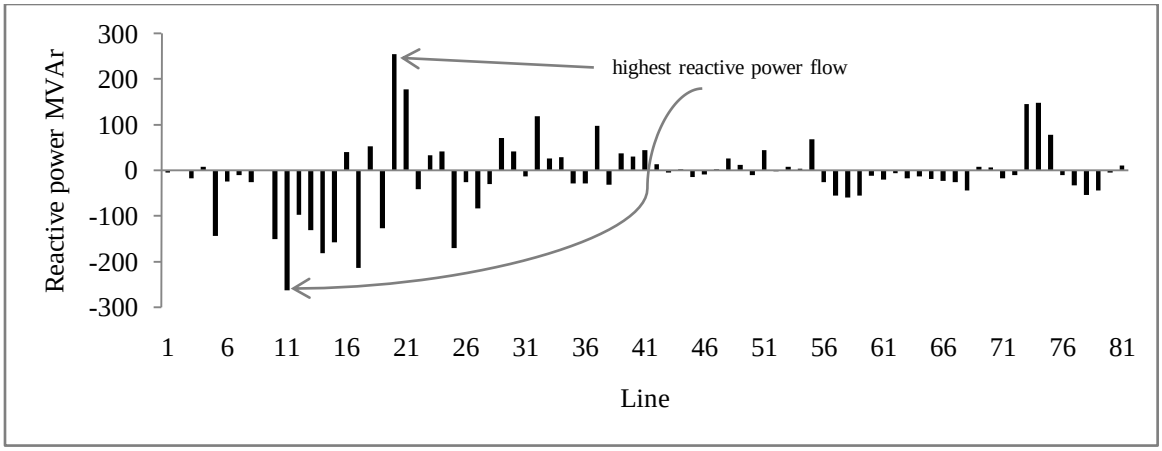

Figure 4.5: Reactive power at base case.

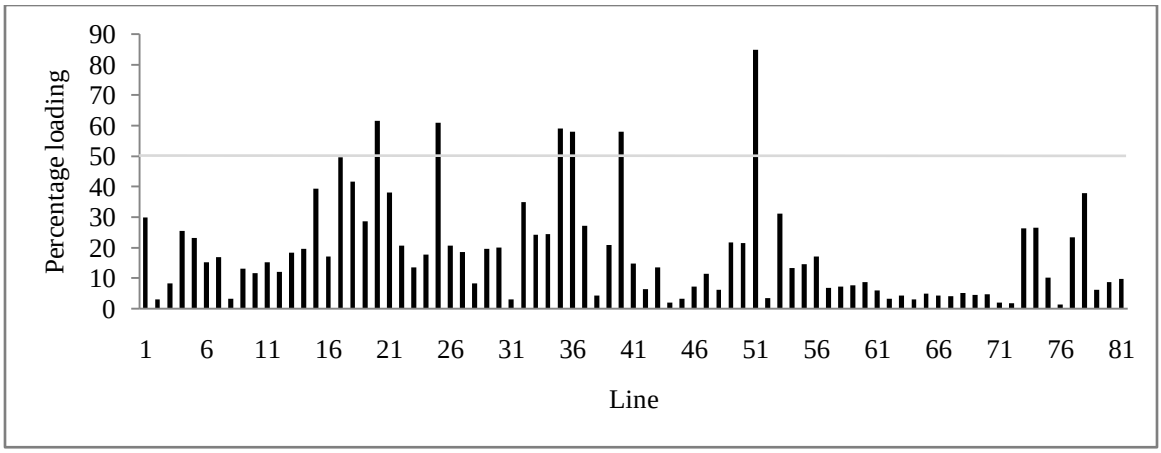

Figure 4.6: Percentage loading at base case.

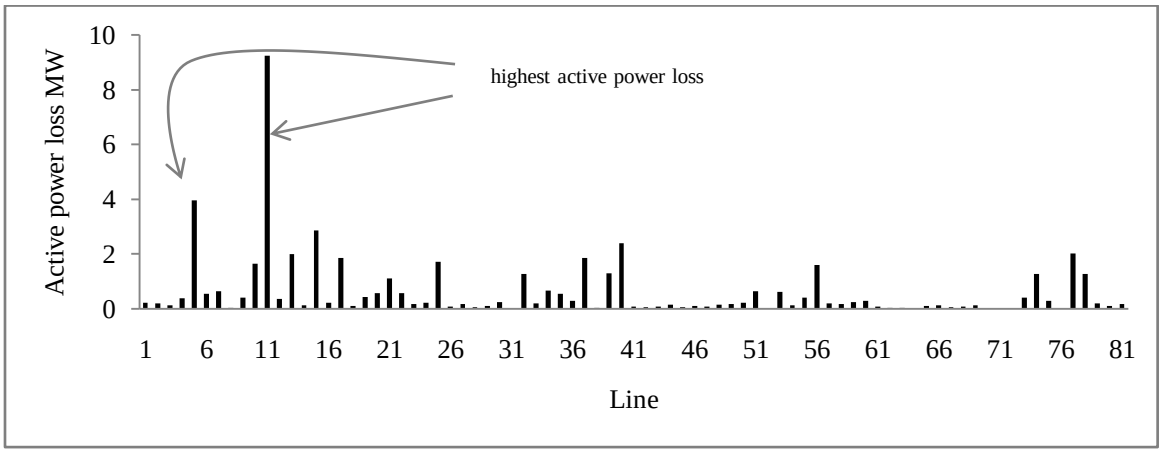

Figure 4.7: Active power losses at base case.

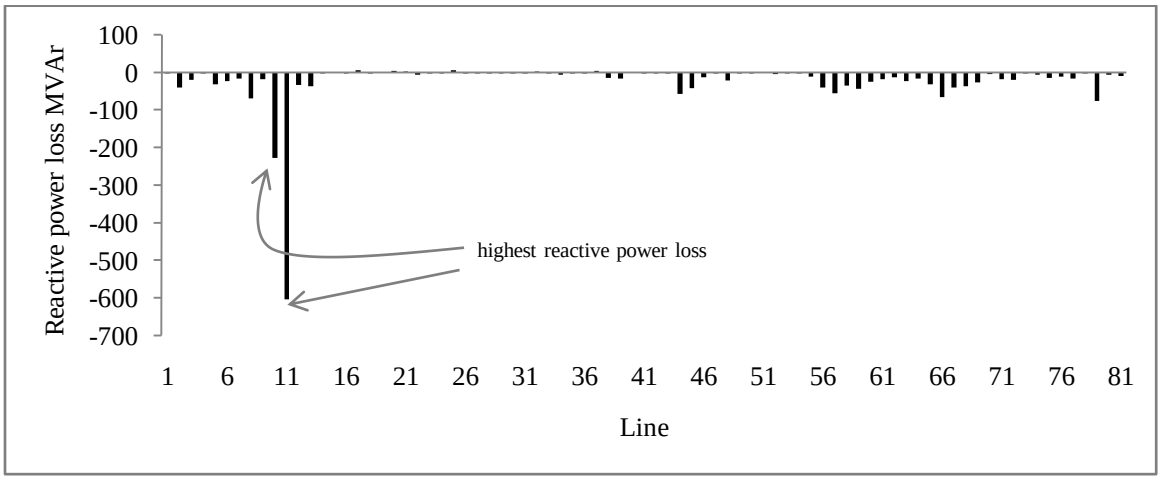

Figure 4.8: Reactive power losses at base case.

The problem of line overloading, voltage drops and transmission losses becomes serious problem during the heavy load conditions. The reason is that the generated power is transmitted through the grid in an inappropriate way. The optimally located FACTS devices bush the system toward its optimal power flow profile.

4.2 Optimal locations for UPFC devices

Line stability index L_{mn} is used to identify the best candidate locations for UPFC installation. The load of the system is increased gradually until reach the collapse point to verify the unstable lines at high loading conditions. Table 4.3 shows the L_{mn} value of lines at different loading conditions, from base case to the collapse point at loading λ_{max}=1.94.

Table 4.3: Line stability index with system loading

Line	**Line stability index L_{mn} with system loading**					
	λ=1	**λ=1.2**	**λ=1.4**	**λ=1.6**	**λ=1.8**	**λ_{max}=1.94**
1	0.004	0.003	0.002	0.001	0.000	0.001
2	0.212	0.229	0.252	0.283	0.336	0.403
3	0.012	0.035	0.061	0.093	0.137	0.243
4	0.078	0.045	0.002	0.061	0.176	0.454
5	0.240	0.287	0.347	0.424	0.533	0.645
6	0.032	0.094	0.167	0.255	0.377	0.867
7	0.005	0.064	0.143	0.238	0.369	1.000
8	0.079	0.086	0.095	0.108	0.131	0.069
9	0.004	0.053	0.129	0.239	0.436	0.902
10	0.154	0.130	0.100	0.061	0.006	0.049
11	0.232	0.252	0.278	0.311	0.358	0.252
12	0.028	0.028	0.028	0.028	0.027	0.024
13	0.135	0.176	0.226	0.290	0.375	0.460
14	0.009	0.013	0.017	0.023	0.030	0.037

15	0.052	0.050	0.048	0.045	0.044	0.043
16	0.022	0.027	0.031	0.036	0.041	0.046
17	0.008	0.010	0.012	0.014	0.015	0.017
18	0.115	0.129	0.144	0.162	0.183	0.244
19	0.032	0.049	0.069	0.092	0.121	0.164
20	0.055	0.069	0.086	0.104	0.126	0.144
21	0.073	0.103	0.135	0.172	0.214	0.306
22	0.009	0.011	0.012	0.013	0.014	0.016
23	0.024	0.030	0.036	0.043	0.052	0.062
24	0.025	0.031	0.037	0.045	0.053	0.063
25	0.167	0.221	0.284	0.361	0.459	0.550
26	0.002	0.002	0.007	0.013	0.020	0.026
27	0.029	0.023	0.016	0.008	0.002	0.011
28	0.017	0.016	0.014	0.012	0.009	0.006
29	0.014	0.016	0.017	0.019	0.021	0.022
30	0.006	0.011	0.018	0.026	0.035	0.045
31	0.034	0.049	0.065	0.083	0.104	0.135
32	0.068	0.065	0.061	0.055	0.045	0.044
33	0.003	0.007	0.011	0.015	0.022	0.028
34	0.014	0.024	0.036	0.050	0.069	0.097
35	0.135	0.154	0.176	0.201	0.231	0.332
36	0.075	0.087	0.099	0.114	0.132	0.169
37	0.164	0.163	0.161	0.157	0.150	0.142
38	0.015	0.019	0.023	0.029	0.037	0.041
39	0.063	0.067	0.069	0.070	0.069	0.081
40	0.645	0.637	0.630	0.625	0.622	0.624
41	0.010	0.011	0.012	0.013	0.014	0.015
42	0.009	0.012	0.015	0.018	0.021	0.024
43	0.003	0.020	0.041	0.068	0.104	0.139
44	0.002	0.034	0.074	0.127	0.201	0.274
45	0.020	0.009	0.044	0.087	0.143	0.195
46	0.009	0.016	0.024	0.035	0.050	0.066
47	0.012	0.020	0.029	0.040	0.053	0.065
48	0.052	0.074	0.101	0.135	0.179	0.220
49	0.082	0.055	0.022	0.019	0.072	0.121
50	0.111	0.051	0.021	0.109	0.221	0.323

51	0.049	0.032	0.011	0.012	0.040	0.065
52	0.038	0.032	0.025	0.018	0.011	0.064
53	0.159	0.192	0.226	0.260	0.294	0.383
54	0.077	0.086	0.095	0.103	0.111	0.087
55	0.045	0.054	0.063	0.076	0.091	0.106
56	0.112	0.085	0.053	0.013	0.037	0.081
57	0.001	0.000	0.002	0.004	0.005	0.081
58	0.020	0.025	0.032	0.040	0.050	0.059
59	0.017	0.018	0.056	0.097	0.142	0.142
60	0.035	0.090	0.151	0.219	0.298	0.413
61	0.006	0.017	0.042	0.074	0.113	0.128
62	0.010	0.025	0.042	0.063	0.090	0.105
63	0.018	0.024	0.031	0.040	0.053	0.001
64	0.005	0.006	0.008	0.010	0.013	0.013
65	0.012	0.035	0.060	0.088	0.121	0.135
66	0.044	0.051	0.058	0.064	0.070	0.047
67	0.024	0.018	0.010	0.001	0.010	0.020
68	0.008	0.005	0.002	0.001	0.004	0.036
69	0.001	0.001	0.001	0.001	0.001	0.001
70	0.028	0.026	0.024	0.022	0.019	0.005
71	0.005	0.006	0.007	0.008	0.009	0.001
72	0.000	0.000	0.000	0.000	0.000	0.009
73	0.009	0.007	0.005	0.001	0.004	0.010
74	0.032	0.025	0.017	0.004	0.014	0.033
75	0.022	0.039	0.061	0.089	0.127	0.164
76	0.000	0.000	0.000	0.000	0.000	0.004
77	0.015	0.007	0.033	0.065	0.106	0.168
78	0.006	0.000	0.007	0.015	0.025	0.038
79	0.119	0.096	0.069	0.039	0.004	0.026
80	0.063	0.102	0.146	0.198	0.259	0.188
81	0.003	0.012	0.022	0.037	0.056	0.078

The lines are rearranged according to L_{mn} value from highest to lowest and shown in table 4.4. This arrangement represents the most severe lines in the system which are the candidate locations for UPFC's installation.

Table 4.4: Ranking of lines severity

Rank	Line	L_{mn}	Rank	Line	L_{mn}
1	7	1.0000	42	8	0.0691
2	9	0.9019	43	46	0.0657
3	6	0.8672	44	47	0.0646
4	5	0.6452	45	51	0.0646
5	40	0.6237	46	52	0.0636
6	25	0.5497	47	24	0.0631
7	13	0.4601	48	23	0.0618
8	4	0.4536	49	58	0.0587
9	60	0.4132	50	10	0.0493
10	2	0.4026	51	66	0.0467
11	53	0.3825	52	16	0.0464
12	35	0.3322	53	30	0.0446
13	50	0.3228	54	32	0.0436
14	21	0.3061	55	15	0.0429
15	44	0.2739	56	38	0.0411
16	11	0.2517	57	78	0.0383
17	18	0.2438	58	14	0.0375
18	3	0.2428	59	68	0.0359
19	48	0.2196	60	74	0.0326
20	45	0.1954	61	33	0.0285
21	80	0.1883	62	26	0.0262
22	36	0.1686	63	79	0.0258
23	77	0.1676	64	42	0.0243
24	75	0.1645	65	12	0.0238
25	19	0.1639	66	29	0.0225
26	20	0.1440	67	67	0.0200
27	59	0.1423	68	17	0.0170
28	37	0.1418	69	22	0.0158
29	43	0.1389	70	41	0.0150
30	31	0.1355	71	64	0.0133
31	65	0.1350	72	27	0.0110
32	61	0.1285	73	73	0.0096
33	49	0.1212	74	72	0.0090
34	55	0.1057	75	28	0.0059
35	62	0.1052	76	70	0.0053
36	34	0.0966	77	76	0.0037
37	54	0.0872	78	71	0.0013
38	39	0.0812	79	1	0.0010
39	56	0.0812	80	63	0.0008
40	57	0.0811	81	69	0.0005
41	81	0.0782			

According to the installation criterion discussed in the previous chapter, seven UPFC devises is installed, the selected UPFC's location are shown in table 4.5.

Table 4.5: Selected places for UPFC installation

Rank	Line	From bus	To bus	L_{mn}
1	7	MWT2	DEB2-B1	1.000164244
2	9	DEB2-B2	DON2	0.90185929
3	5	ATB2	SHN2	0.645191638
4	40	OHAS1	GAD B2	0.623671911
5	25	KLX1	KUK1	0.549721636
6	60	UMR2	OBD2	0.413167239
7	53	SNP1	MIN1	0.382504059

Table 4.6: Parameters of installed UPFC's

Name	Line	P set	Q set	Vs set	Vr min	Vr max
		MW	MVAr	V	%	%
UPFC-1	7	-53.4	-11.1	1	0.9	1.1
UPFC-2	9	-43.7	-17.3	1.026	0.9	1.1
UPFC-3	5	-0.4	-121.5	0.954	0.9	1.1
UPFC-4	40	9.6	31.5	1.007	0.9	1.1
UPFC-5	25	142.1	132.7	0.986	0.9	1.1
UPFC-6	60	38.2	-15	1	0.9	1.1
UPFC-7	53	-14	8.2	0.998	0.9	1.1

Optimal power flow is done and the results at the candidate locations are used to set the power flow parameters for the UPFC's, table 4.6 shows the control value for the active and reactive line flow and the control value for the voltage magnitude of the sending bus for the seven UPFC devices.

4.3 System improvements after installing the UPFC devices

Table 4.7 shows the bus voltages and angles after installing the UPFC's and table 4.8 shows the load flow result after installing the UPFC's.

Table 4.7: Bus voltage and angle after installing UPFC devices

Bus number	Bus name	Per Unit Voltage		Angle Degree	
		with	without	with	without
1	MWP500	1	1	0	0
2	ATB5	1.0213	1.0031	-1.6	-3.7
3	MRK5	0.9691	0.9777	-9.2	-7.6
4	KAB5	0.9708	0.9799	-10.1	-8.3
5	WHL2	0.9895	0.9892	-5.3	-8.7
6	WWA2	1.0208	1.0204	-4.6	-8
7*	DEB2-B1	1	1.0216	-2.6	-6.2
8	DEB2-B2	1.038	1.0443	-5.1	-5
9*	DON2	1.026	1.0256	-4.3	-7.7
10	MWT2	1.0181	1.0315	-2.7	-2.8
11	MWP2	1.0327	1.0384	-1.5	-1.5
12*	ATB2	0.954	0.924	-3.7	-9.1
13	SHN2	0.9696	0.9688	-21.8	-13.8
14	MRK2	1.0007	1.0051	-22.8	-19.4
15	GAM2	0.9807	0.9844	-23.9	-20.4
16	KAB2	0.9851	0.9871	-21.1	-16.6
17	FRZ2	0.9974	0.9976	-21.5	-16.4
18	GER2	1	1	-21.5	-16.4
19	IBA2	0.9922	0.9951	-23.1	-18.6
20	MHD2	1.0002	1.0045	-23.5	-20
21	KLX2	0.9901	0.9938	-23.7	-19.4
22	JAS2	0.9771	0.9812	-24.5	-20.8
23	GAD2	0.9759	0.9831	-24.9	-21
24	SOB2	0.987	0.9914	-24	-19.8
25	NHAS2	0.9689	0.9574	-27.2	-23.5
26	MAR2	0.9637	0.9559	-27.8	-24.2
27	MSH2	0.9943	0.996	-24.3	-20.6
28	RBK2	1	1	-23.8	-20.1
29	SNJ2	0.9755	0.971	-27.3	-23.7
30	SNG2	0.9923	0.9893	-26.7	-23.1
31	ROS2	1	1	-22.1	-18.5
32	RNK2	1.0079	1.0079	-23	-19.4
33	HWT2	1.0005	0.9983	-27.3	-23.7
34	OBD2	0.9887	0.9987	-25.1	-23.2

35*	UMR2	1	1.0054	-25.2	-21.6
36	TND2	1.004	1.0072	-24.7	-21.1
37	DBT2	0.9914	1.0019	-25.8	-23.9
38	ZBD2	0.9899	1.0006	-26.1	-24.1
39	FUL2	0.9917	1.0026	-26.5	-24.6
40	BBN2	0.9937	1.0046	-26.6	-24.7
41	GDF2	0.9996	0.9983	-27.7	-24.2
42	GRB2	0.9927	0.9916	-28.2	-24.6
43	SHK2	0.9992	0.9978	-27.8	-24.2
44	NHLF2	0.9925	0.9914	-28.3	-24.7
45	ARO2	0.9994	0.9982	-28.5	-25
46	KSL2	0.9984	0.9972	-28.5	-25
47	HUD	0.9959	1.0002	-23	-19.6
48	UTP2	0.9996	0.9983	-27.8	-24.2
49	SHD2	1	1	-26.5	-23
50	KHE1	0.9833	0.9821	-33.5	-26.8
51	IZB1	0.9661	0.9663	-31.6	-25.7
52	IBA1	0.9733	0.9734	-31.1	-25.3
53	KHN1	1	1	-32.5	-26.4
54*	KUK1	0.986	0.9848	-33.3	-26.6
55	IZG1	0.9777	0.975	-31.6	-26.3
56	MHD1	0.969	0.9642	-30.6	-25.9
57	FAR1	0.9547	0.9288	-29.2	-26.8
58	AFR1	0.9621	0.9364	-28.8	-26.4
59	KLX1	0.9694	0.944	-28.4	-26
60	LOM1	0.9674	0.9441	-28.8	-26.2
61	SHG1	0.9695	0.9516	-29.3	-26.3
62	MUG`	0.967	0.9547	-30.1	-26.5
63	BNT1	0.9688	0.9585	-30.2	-26.4
64	OMD1	0.9658	0.9576	-30.6	-26.4
65	GAM1	0.9937	0.9858	-29.2	-25.5
66	JAS1	1.0133	1.0035	-27.9	-24.7
67	BAG1	0.9983	0.9203	-28.9	-24
68	SOB1 B2	0.9798	0.9355	-28.6	-25.3
69*	GAD B2	1.007	0.924	-28.8	-23.6
70	NHAS1	1.0275	1.0349	-28.7	-25.7
71	OHAS1	1.0277	1.0317	-28.9	-25.9
72	GND1	1.0244	1.0284	-29.1	-26.1
73	MAR1 B1	1.0334	1.0291	-30.3	-26.8
74	MAN1	1.023	1.0186	-31.2	-27.6
75	ORBK1	1.0205	1.0197	-28.7	-25.2
76	SNJ 1	1.0209	1.0201	-28.6	-25.1
77	HAG1	1.0143	1.0116	-29.8	-26.3
78	SNP1	1	1	-28.2	-24.8
79*	MIN1	0.998	0.9481	-28.2	-25.8
80	FAO1	1.0085	1.0049	-30.7	-27.2
81	GDF 1	1.0182	1.0165	-29.1	-25.5
82	GRB6	1	1	-29	-25.5

* denotes the controlled voltage bus by UPFC's denotes the busses near to the voltage limits.

Table 4.8: Power flow results after installing UPFC devices

Line	From bus	To bus	P MW	Q MVAr	Loading %	P Loss MW		Q Loss MVAr	
						with	without	with	without
1	69	67	46.554	45.724	40.01	0.3627	0.2022	0.3402	0.1612
2	6	5	14.547	0.56	2.99	0.1867	0.1867	-40.2986	-40.2693
3	7	9	21.446	-35.613	12.84	0.2492	0.106	-18.2981	-19.4675
4	11	10	85.202	34.675	27.5	0.4397	0.373	-2.6511	-3.0979
5*	12	13	1.487	76.564	8.29	1.0874	3.9588	-44.9362	-31.9876
6	11	8	44.654	-23.427	15.08	0.5398	0.537	-22.697	-23.0091
7*	10	7	1.554	5.731	1.8	0.0519	0.629	-19.1509	-16.7687
8	9	6	14.577	-26.692	3.11	0.0302	0.0302	-68.9311	-68.8835
9*	8	9	44.114	-0.729	13.12	0.4139	0.4089	-18.0294	-18.3098
10	1	2	101.427	-211.871	9.39	0.4887	1.6304	-243.638	-227.912
11	1	3	826.737	-212.039	17.63	13.6423	9.2555	-554.905	-604.129
12	3	4	362.259	-91.766	15.41	0.6	0.3596	-29.6582	-32.6829
13	13	17	35.339	55.346	6.91	0.5875	1.9928	-41.8331	-36.1638
14	17	18	18.825	178.783	18.87	0.1131	0.1179	-1.5268	-1.5076
15	16	19	331.028	-147.453	38.61	2.7739	2.8673	0.8559	1.2191
16	52	51	68.208	39.775	17.03	0.2018	0.2017	-0.217	-0.2175
17	52	53	123.338	-223.934	55.15	2.2834	1.8548	8.0074	6.2865
18	54	50	82.004	53.169	41.62	0.0872	0.0874	0.042	0.0436
19	56	55	148.967	-131.647	43.07	0.93	0.4105	2.9815	0.9014
20	53	54	269.579	216.529	75.62	0.8542	0.5689	6.3974	4.1539
21	53	55	73.848	-181.19	42.01	1.3233	1.1016	4.1477	3.2608
22	14	20	219.1	-48.47	23.54	0.7253	0.5546	-5.4355	-6.1948
23	58	57	50.419	32.591	13.1	0.1527	0.1614	-0.6637	-0.561
24	59	58	67.826	40.871	17.15	0.2046	0.2164	-0.1972	-0.0968
25*	59	54	142.1	132.7	64.98	1.965	1.7158	7.5303	6.4934
26	59	60	181.366	12.456	39.37	0.2921	0.0793	0.8935	0.0529
27	60	61	95.73	-46.456	23.09	0.2605	0.1679	0.3194	-0.0219
28	61	62	105.033	-6.1	22.78	0.3585	0.0456	0.4154	-0.8095
29	63	62	29.208	-49.082	12.4	0.0365	0.0916	-0.2069	0.0225
30	56	64	4.136	-31.14	6.83	0.0265	0.2351	-0.7573	0.095
31	64	63	85.586	23.293	19.22	0.1372	0.0032	0.0025	-0.5247
32	65	63	116.638	105.817	33.27	1.1554	1.2724	3.061	3.5599
33	21	24	120.524	51.007	20.4	0.1383	0.1945	-1.9476	-1.6716
34	24	23	120.385	52.955	20.57	0.473	0.651	-6.2126	-5.3725
35	67	68	9.701	21.147	42.62	0.2877	0.5314	-0.2276	0.1362
36	68	59	9.414	21.375	43.59	0.1654	0.2876	-0.1104	0.0593
37	66	61	75.831	82.358	23.19	1.3527	1.851	1.6229	3.7283
38	22	23	57.145	-9.137	6.22	0.0854	0.0294	-13.2929	-13.6741
39	23	25	106.706	-9.983	16.95	0.8073	1.2962	-18.0289	-15.3411
40*	71	69	9.6	20.318	37.36	1.0417	2.3977	-1.592	0.4865

41	70	71	37.44	-13.302	8.12	0.0206	0.0681	-0.4415	-0.2566
42	71	72	27.859	12.837	6.27	0.0378	0.0375	-1.4161	-1.4297
43	71	73	7.03	-9.652	21.25	0.1875	0.0746	-1.6828	-1.8188
44	27	22	20.183	7.604	2.28	0.1807	0.1374	-56.2806	-56.7841
45	28	27	27.239	-8.932	3.01	0.0664	0.0518	-42.0699	-42.201
46	25	26	43.729	6.904	7.05	0.097	0.0898	-13.5742	-13.3328
47	73	74	10.954	1.714	11.26	0.0684	0.069	-2.3441	-2.321
48	29	26	27.339	16.79	5.08	0.1052	0.1493	-21.1059	-20.6009
49	73	77	3.183	12.997	23.68	0.1841	0.1554	-0.9768	-1.0033
50	78	77	4.831	-11.641	23.05	0.2364	0.2031	-1.7038	-1.7386
51	76	78	17.608	46.687	89.38	0.6914	0.6251	0.5026	0.4227
52	76	75	0.336	-1.793	3.27	0.0004	0.0004	-3.2692	-3.2643
53*	78	79	0.382	-0.61	1.32	0.0008	0.6175	-2.2502	-1.3946
54	73	80	6.854	3.528	13.64	0.1333	0.1263	-2.2585	-2.2482
55	30	29	62.091	62.262	13.68	0.3436	0.3883	-11.4574	-11.1206
56	31	30	105.461	-29.718	16.91	1.5583	1.6	-40.1956	-39.8294
57	31	32	34.206	-56.325	6.92	0.1922	0.1805	-55.2747	-55.3223
58	30	33	29.783	-57.37	6.84	0.1562	0.173	-34.8651	-34.6115
59	28	36	44.532	-45.725	6.7	0.1954	0.2436	-43.4789	-43.4277
60*	35	34	1.396	3.176	0.73	0.0433	0.2737	-24.5682	-24.026
61	34	37	19.796	-18.906	5.81	0.0627	0.064	-17.0753	-17.4264
62	37	38	13.483	-5.769	3.11	0.0169	0.0165	-12.7974	-13.0728
63	38	39	10.106	-16.736	4.15	0.0216	0.0216	-23.1172	-23.6209
64	39	40	3.364	-12.942	2.83	0.0043	0.0044	-15.4452	-15.7832
65	36	35	43.329	-7.806	4.6	0.1043	0.1017	-30.8051	-31.0856
66	32	28	33.611	-23.435	4.27	0.1354	0.1251	-64.7106	-64.7524
67	33	41	28.08	-23.463	3.84	0.0554	0.0585	-39.5015	-39.346
68	42	46	16.729	-43.807	4.96	0.0611	0.0609	-37.1522	-37.0655
69	43	42	42.129	8.796	4.52	0.1111	0.1091	-27.1327	-27.0712
70	41	43	42.812	6.979	4.56	0.0109	0.0108	-3.2271	-3.2184
71	46	45	0.002	-17.333	1.82	0.0023	0.0023	-17.3328	-17.2922
72	42	44	12.034	-11.084	1.73	0.005	0.0051	-19.1054	-19.0608
73	14	47	231.737	130.86	27.92	0.4435	0.3937	-1.7816	-2.0127
74	47	15	231.293	132.642	28.1	1.4182	1.2676	-5.1695	-5.8611
75	17	16	30.631	-129.411	14.17	0.4294	0.2754	-13.1077	-13.7576
76	43	48	0.001	-11.105	1.17	0.0006	0.0006	-11.1051	-11.0751
77	18	19	167.175	-4.636	17.56	1.1628	2.0254	-18.9774	-15.5831
78	19	21	261.393	-12.707	27.69	0.6735	1.2541	-2.7588	-0.4641
79	49	41	38	-46.854	6.33	0.2032	0.1984	-76.2074	-76.1212
80	81	80	4.396	-4.49	8.75	0.0956	0.0982	-5.2425	-5.2118
81	15	22	113.237	10.444	12.17	0.2634	0.1694	-9.4705	-9.9772
Total						**46.6929**	**50.1895**	**-1928.76**	**-1943.18**

* denotes UPFC's locations

As expected, the power flows in the UPFC-upgraded network differ with respect to the original case. The most noticeable changes in voltage profile are shown in figure 4.9.

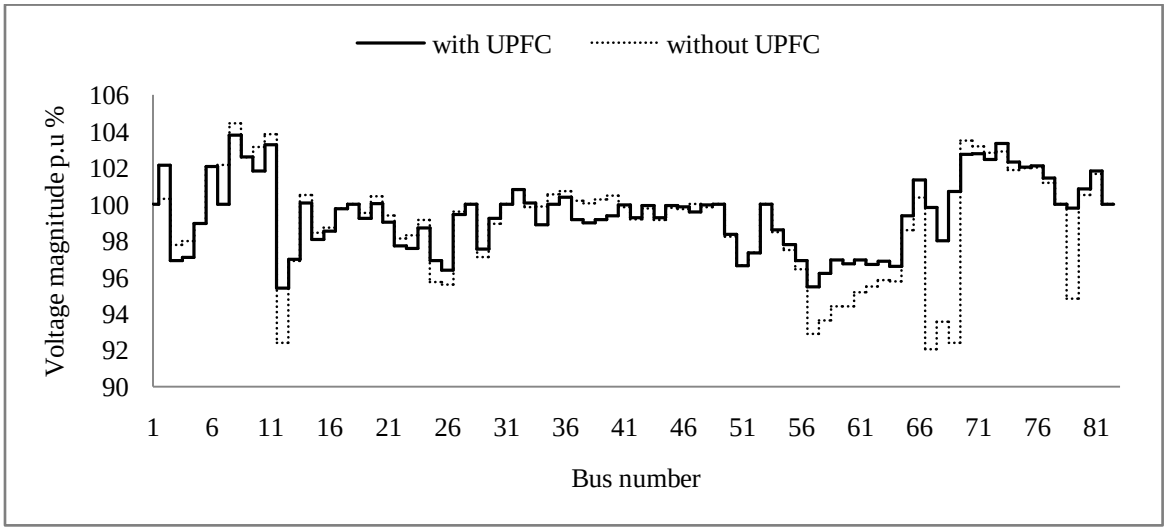

Figure 4.9: Voltage profiles with and without UPFC's.

The overall voltage profile is improved by 35.29%, all the weak busses is improved as shown in figure 4.10.

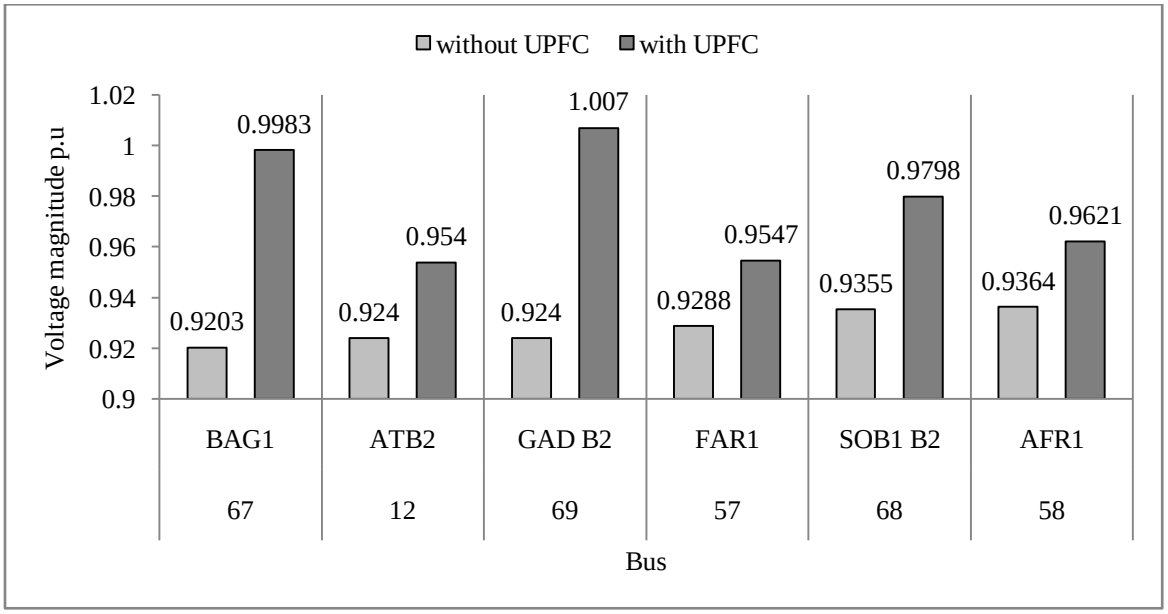

Figure 4.10: Voltage improvements at the weak busses.

The greatest voltage value in the system is become 1.038 p.u at bus 8 (DEB2-B2) with 0.63% decrease from the base value. The weakest voltage is become 0.954 p.u at bus 12 (ATB2) with 3% increase from the base value. It's observed that the entire busses become within $\pm 5\%$ of the nominal voltage.

Figure 4.11 and 4.12 shows the active and reactive power flow with and without UPFC's, the power flow of the system is modified due to the controlled lines flow by UPFC devices.

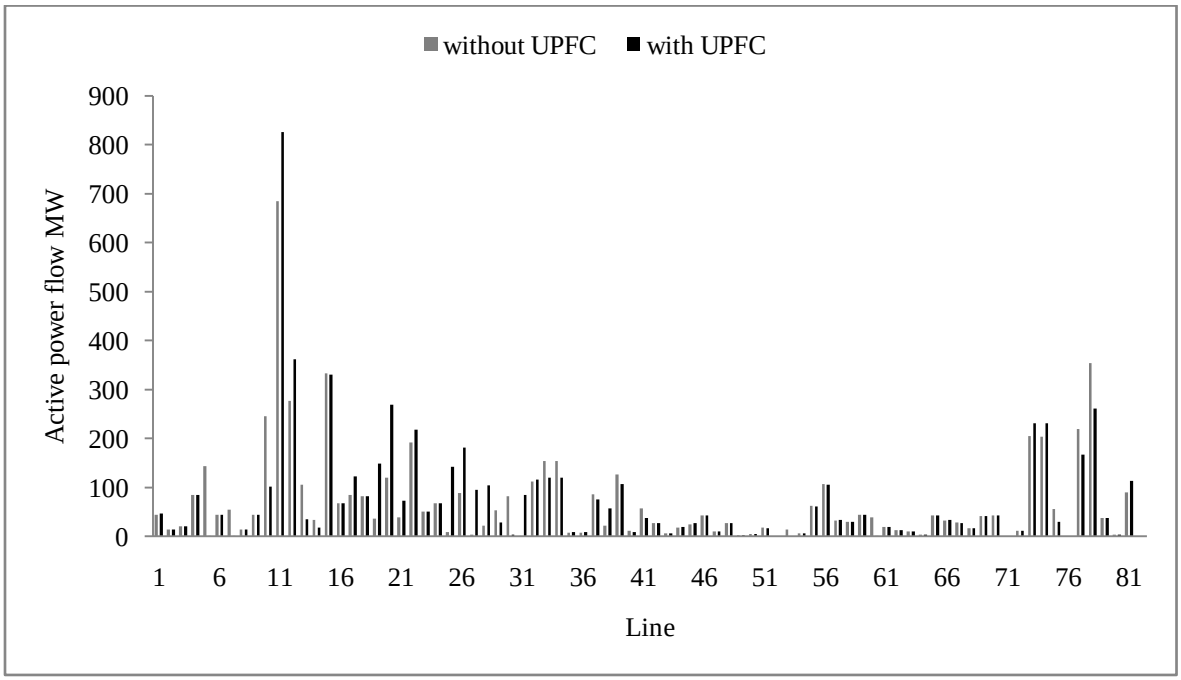

Figure 4.11: Active power with and without UPFC's.

Line 11 (MWP500-MRK5) is caring the highest active and reactive power flow which are 826.737 MW and 216.529 MVAr, it's active power flow increased form the base case by 20.69 %, on the other hand it's reactive power flow decreased from the base case by 19.55 % also the consumed reactive power by Merowe generators is decreased.

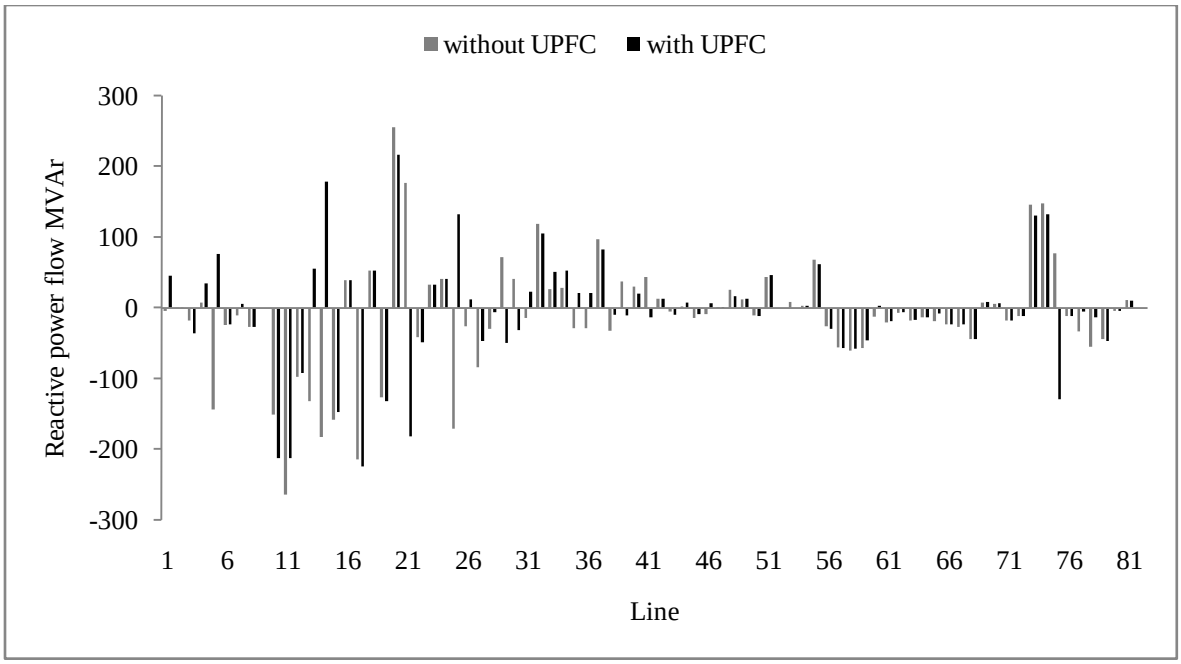

Figure 4.12: Reactive power with and without UPFC's.

Percentage loading of the transmission lines is represented at figure 4.13, although line 11 has the highest power flow value but it's loaded by 17.63% of its maximum rating.

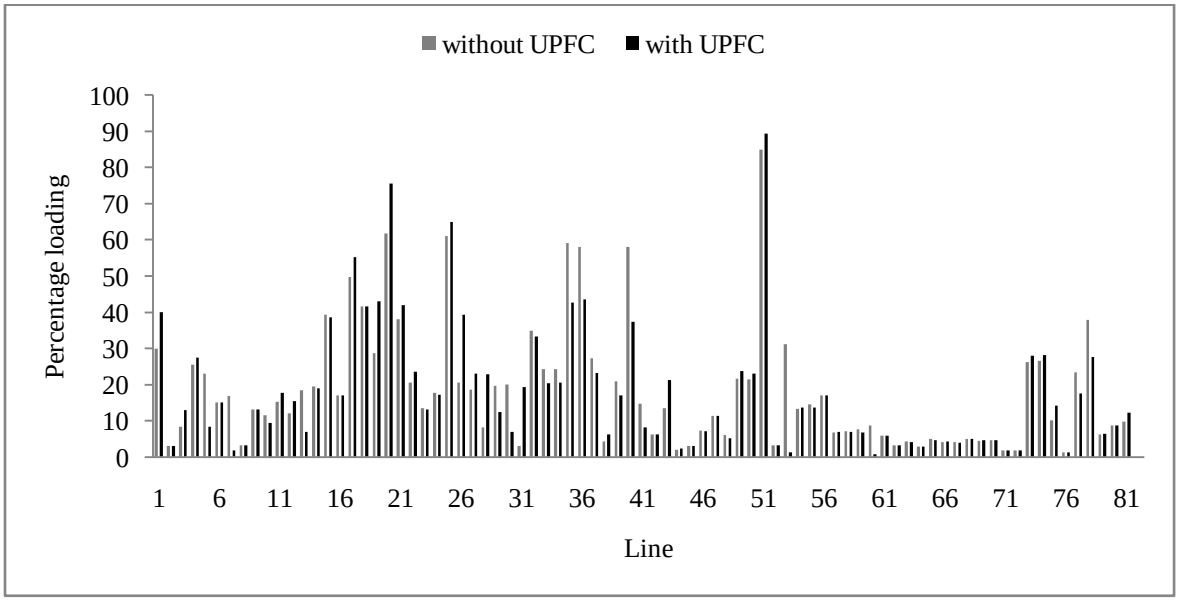

Figure 4.13: Percentage loading with and without UPFC's.

As shown in the previous figure, only four lines are loaded above 50% of its maximum loading rate. The loading of 45 lines is decreased after installing the UPFC devices. The overall loading of the system has been decreased by 3.26 % of the base case loading.

The highest overloading is 89.38% observed at line 51 (SNJ 1-SNP1). Its loading is increased by 4.4% of its base loading, although it is active and reactive power flow is light compared with corresponding lines.

Figure 4.14 and 4.15 shows the active and reactive power losses before and after installing the UPFC devices.

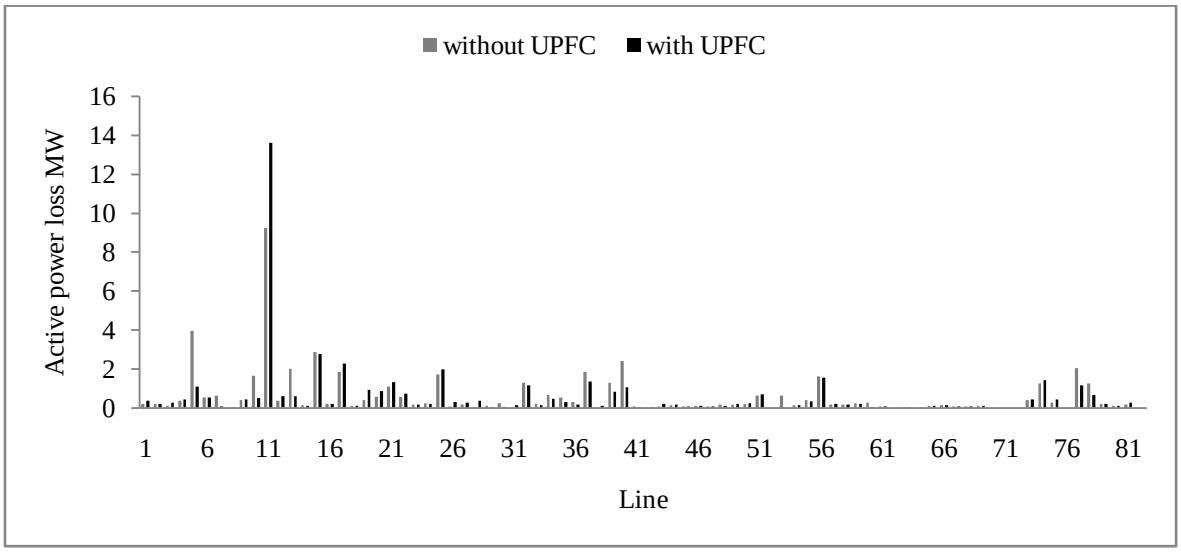

Figure 4.14: Active power losses with and without UPFC's.

The overall active power losses of the system are decreased to 46.6925 MW, highest reduction in active power losses is 2.8714 MW at line 5 (ATB2-SHN2) where UPFC-3 is installed.

The highest active power losses are observed at line 11 (MWP500-MRK5) as a result of its high active power flow value, although the active loss at this line is increased by 4.3868MW the total active losses of the system have been decreased by 3.4966 MW.

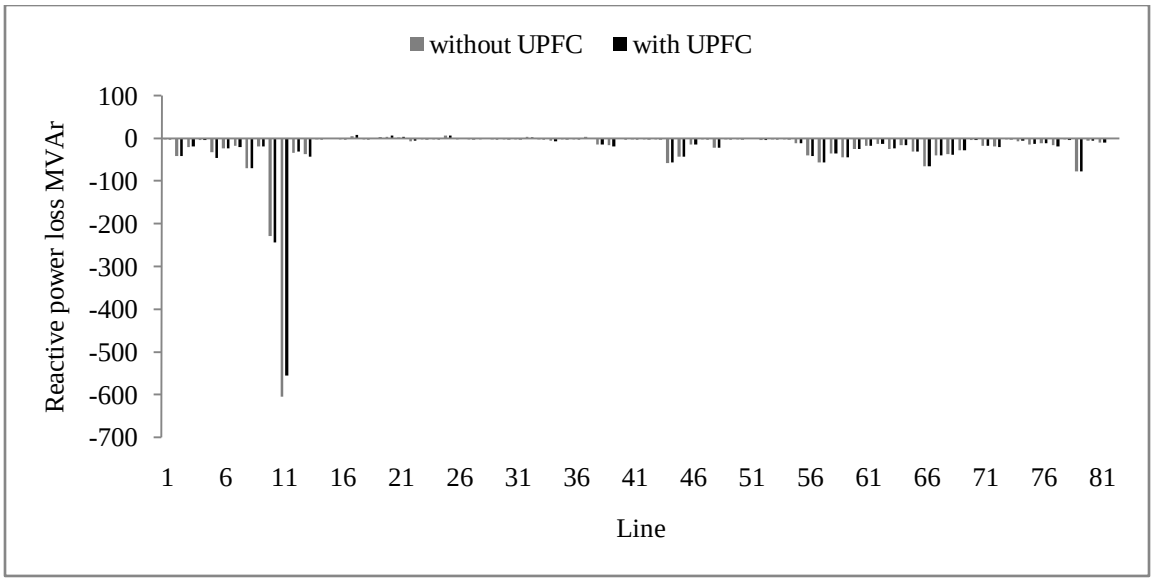

Figure 4.15: Reactive power losses with and without UPFC's.

The overall reactive power losses of the system are decreased to 1928.76 MVAr, The highest reactive power loss is 554.905 MVAr which observed at line 11 (MWP500-MRK5), also this line take the highest reduction in reactive power losses by 49.224 MVAr.

Table 4.9 summarizes the total improvement in power losses in the system at the base case and after installing the UPFC devices. Figures 4.16-4.18 shows the overall power losses improvement and the energy saved by installing the UPFC devices.

Table 4.9: Power flow improvement

Losses	Without UPFC	With UPFC	Saved power	Percentage improvement
Active power MW	50.18995	46.6925	3.49745	6.968427
Reactive power MVAr	-1943.18	-1928.76	14.4218	0.742175

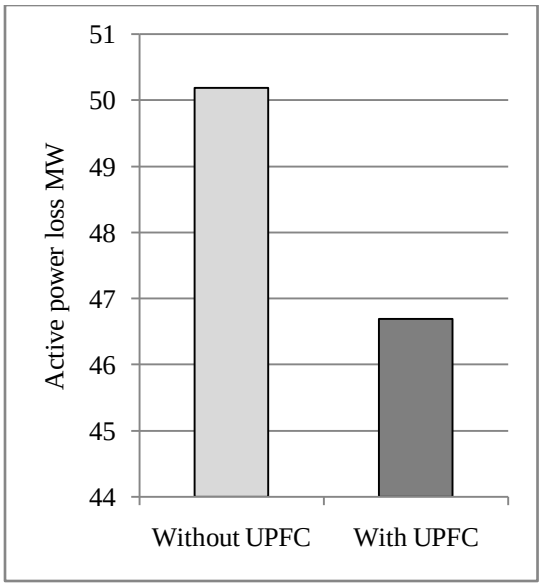

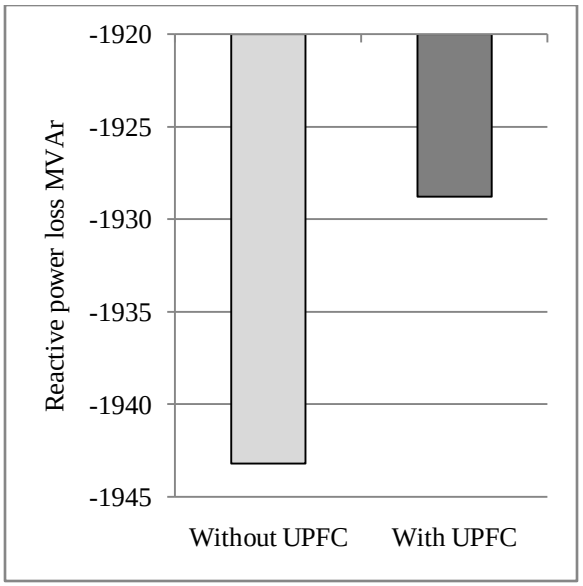

Figure 4.16 Total active power loss

Figure 4.17 Total reactive power loss

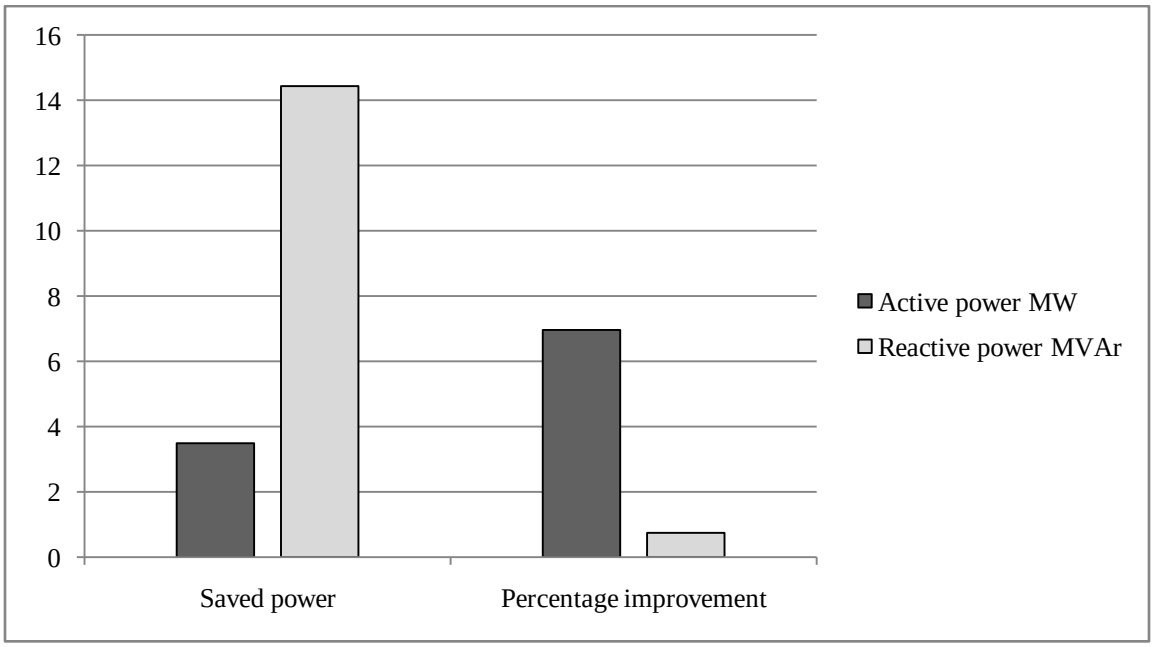

Figure 4.18: Total saved power and percentage improvement.

Figure 4.19 shows the voltage profiles according to number of UPFC devices installed.

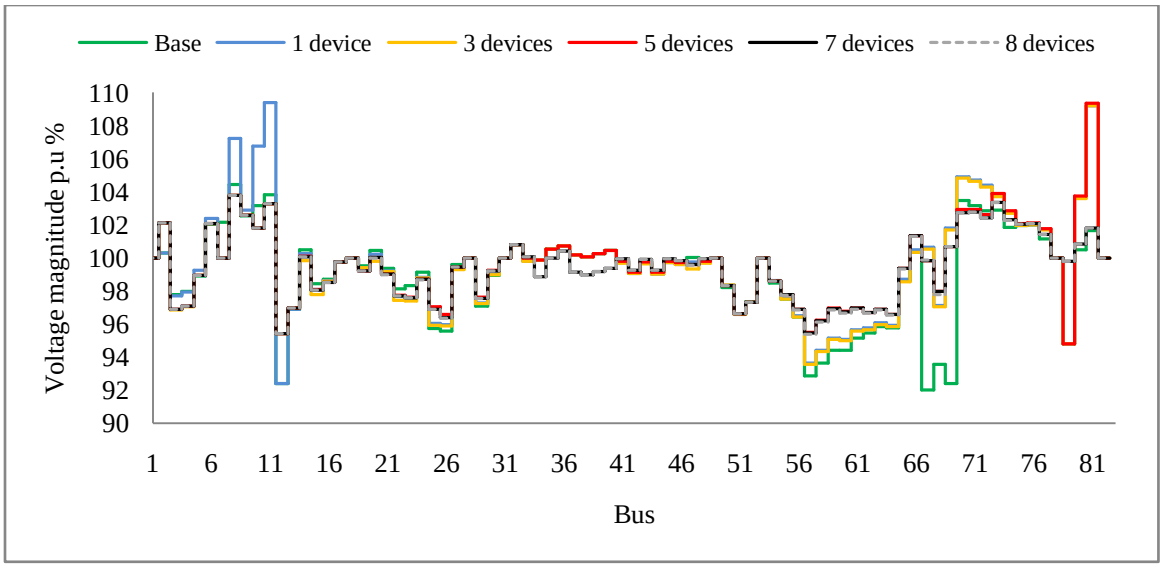

Figure 4.19: Voltage profiles according to number of UPFC devices installed.

The voltage profile when the eighth UPFC device is installed was modified by a narrow margin to that one at installing seven UPFC devices. Table 4.10 shows the power flow improvement according to number of UPFC devices installed and figures 4.20 and 4.21 represents this improvement.

Table 4.10: Power flow improvement according to number of UPFC devices installed

Losses	Base	1 device	3 devices	5 devices	7 devices	8 devices
Active power MW	50.18995	48.8272	48.12453	47.72838	46.6925	46.58394
Reactive power MVAr	-1943.18	-1937.33	-1935.13	-1930.89	-1928.76	-1927.32

The losses improvement after installing the eighth UPFC device was too slight to take it into account.

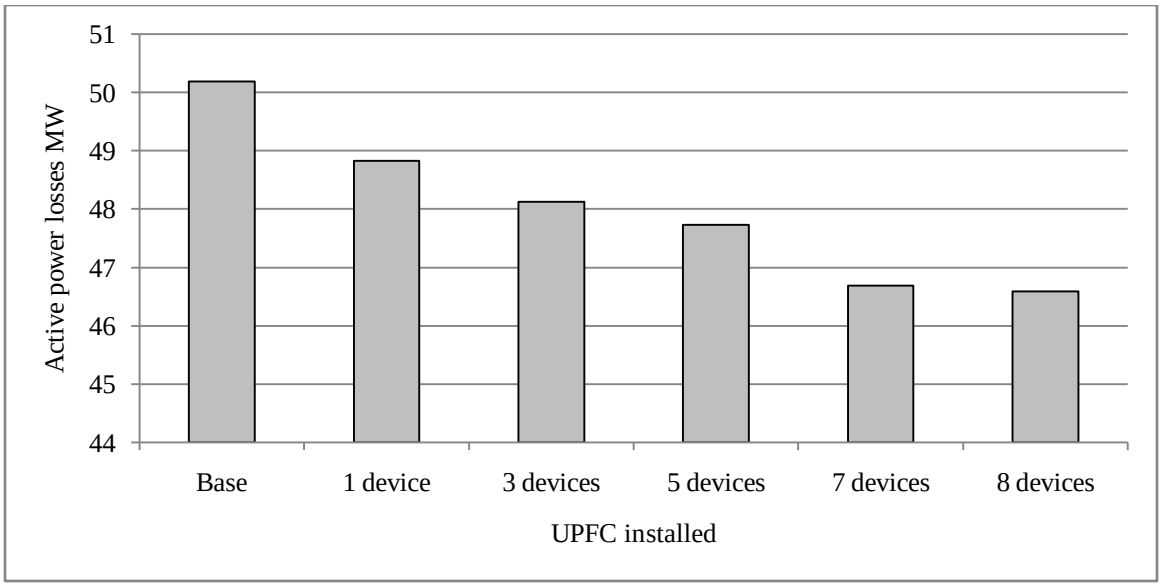

Figure 4.20: Active power losses according to number of UPFC devices installed.

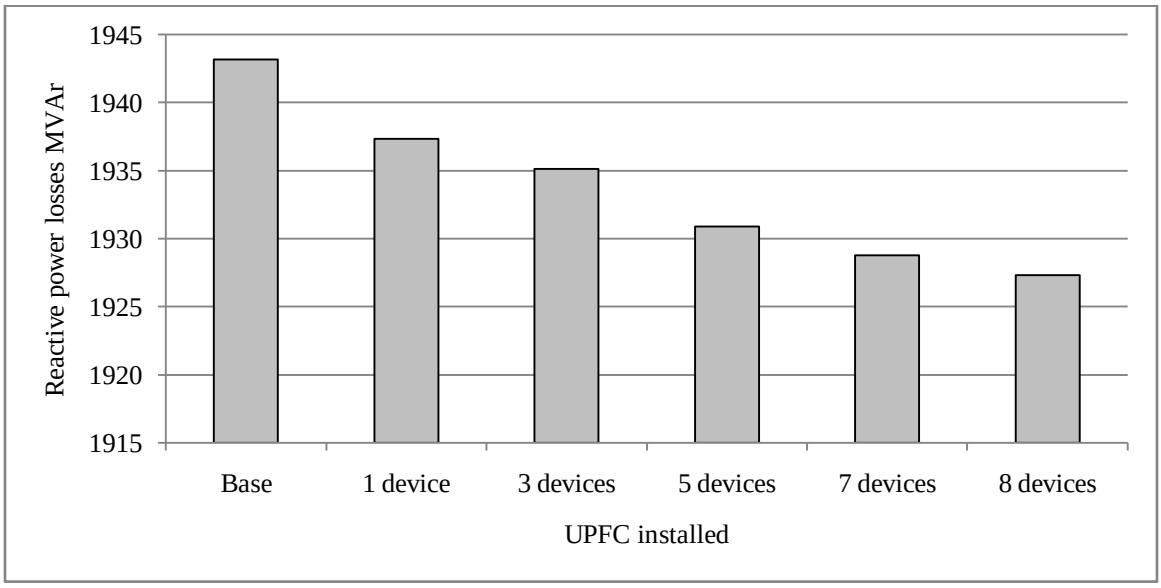

Figure 4.21: Reactive power losses according to number of UPFC devices installed.

CHAPTER FIVE

CONCLUSION AND RECOMMENDATIONS

5.1 Conclusion

In this thesis, method for successful UPFC placement, where the objective is to minimize the line losses and the bus voltage limit violations, is proposed. The method is implemented on a real electrical power grid of Sudan. The optimal locations are achieved by considering of the line stability index L_{mn} at heavy active and reactive power loading.

An optimal power flow OPF formulation considering the minimization of active power losses as an objective has been developed to set the power flow parameters for the UPFC and push the system toward its optimal power flow profile.

NEPLAN software is used to simulate the Sudanese electrical network and obtain the power flow results. Seven devices are the optimal number of UPFC devices in this study, and the devices are installed in the system providing the following improvement conclusion:

- The overall voltage profile is improved by 35.29%, the bus voltage limit violations are confined within $\pm 5\%$ of the nominal voltage.
- Total energy saved by installing the UPFC devices is 3.49745 MW and 14.4218 MVAr.
- Total active and reactive losses of the system have been decreased by 6.96% and 0.74% of the base case, respectively.

5.2 Recommendations

Further development in this area is recommended for research as follows:

- In this thesis, optimal placement of only UPFC devices has been studied. This can be extended for the placement of some other types of FACTS series controllers, such as TCSC, TCPAR and SSSC.
- Such criteria can be extended to various shunt devices such as SVC and STATCOM.
- Economic aspects such as FACTS device cost can be compared with the price to be paid while the system at base condition, this can result into a new formulation.
- Various models for the loads in the system can be taken into account.
- Only static criteria have been used in this thesis for the optimal placement of UPFC devices. A set of hybrid indices can be developed using both static and transient criteria.
- Besides static analysis, dynamic performance should also be checked.
- For optimal locating of UPFC a line stability index L_{mn} has been used. There are other indices that verify the weak points of the system. These indices can be tried out.
- Some of the evolutionary optimization methods are used in optimal FACTS placement such as Genetics Algorithm GA, Particle Swarm Optimization PSO and other Artificial Intelligence AI based methods, this can be applied as a future research work.

REFERENCES

[1] E. Acha, C. R. Fuerte-Esquivel, H. Ambriz-Perez, and C. Angeles-Camacho, *"FACTS: Modelling and Simulation in Power Networks"*, Chichester, U.K.: Wiley, 2004.

[2] Y. H. Song, A. T. Johns, "*Flexible AC Transmission Systems (FACTS)"*, IET, 2009.

[3] N. G. Hingorani, L. Gyugyi, *"Understanding FACTS"*, IEEE Press, 2001.

[4] K. R. Padiyar, *"Facts: Controllers in Power Transmission and Distribution"*, Bangalore, India, Anshan, 2007.

[5] J.A. Momoh, S. Surender Reddy, *"Optimal Location of FACTS for ATC Enhancement"*, IEEE, 2012.

[6] Kalyan K. Sen, Mey Ling Sen, *"Introduction to FACTS Controllers Theory, Modeling, and Applications"*, IEEE Press Series on Power Engineering-Wiley-IEEE Press, 2009.

[7] E. Acha, V.G. Agelidis et al., *"Power Electronic Control in Electrical Systems"*, Newnes Power Engineering SERIES, 2002.

[8] F. Ghezal, J.M Ramirez et al, *"The two modes of 48-pulses StatCom"*, International Conference on Electrical Networks, 2010.

[9] Xi-FanWang, Yonghua Song, and Malcolm Irving. *"Modern Power System Analysis"*, Springer, 2008.

[10] Anju Gupta, P.R.Sharma, *"Optimal Placement of FACTS Devices for Voltage Stability Using Line Indicators"*, IEEE, 2012.

[11] E.Z.Yahia, M.A.Elsherif , M.N.Zaggout, *"Detection of Proximity to Voltage Collapse by Using L –Index"*, International Journal of Innovative Research in Science Engineering and Technology, 2015.

[12] Shiwani Rai, P.S.Venkataramu, M.S.Nagaraja, *"Line Congestion Relief Using UPFC"*, International Conference on Power, Energy and Control, 2013.

[13] Shameem Ahmad, Hazlie Mokhlis et al, *"A Placement Method of Fuzzy based Unified Power Flow Controller to Enhance Voltage Stability Margin"*, IEEE, 2014.

[14] Neena Ramesh, B.V. Sanker Ram et al, *"Voltage/Line Stability Indices Assessment in a Strategic Dispatch of Maximum Reactive Power with UPFC"*, International Conference on Sustainable Energy and Intelligent System, 2011.

[15] S.Pérez-Londono, L.F.Rodriguez, G.Olivar, *"A Simplified Voltage Stability Index (SVSI)"*, Electrical Power and Energy Systems, 2014.

[16] F.A.Althowibi, M.W.Mustafa, "*Voltage Stability Calculations in Power Transmission Lines: Indications and Allocations"*, IEEE,International Conference on Power and Energy, 2010.

[17] Omorogiuwa Eseosa1, F.O.Odiase, *"Efficiency Improvement of Nigeria 330KV Network Using Flexible Alternating Current Transmission System (FACTS) Devices"*, International Journal of Advances in Engineering & Technology, 2012 .

[18] Esmaeil Ghahremani and Innocent Kamwa, *"Optimal Placement of Multiple-Type FACTS Devices to Maximize Power System Loadability Using a Generic Graphical User Interface"*, IEEE, 2012.

[19] M. W. Mustafa, R. O. Bawazir, *" Optimal Location of Facts for ATC Enhancement"*, International Journal of Engineering and Advanced Technology, 2013.

[20] Abdelaziz Laïfa, Mohamed Boudour, *"Optimal Placement and Parameter Settings of Unified Power Flow Controller Device using a Perturbed Particle Swarm Optimization"*, International Conference on Electrical Networks, 2010.

[21] M.Tümay, A.Mete Vural, K.L.Lo, *"Simulation of Unified Power Flow Controller by Using Modified Power Injection Model"*, Iranian Journal of Science & Technology, Transaction and Engineering, 2005.

[22] Adepoju G. A. Komolafe, O.A Aborisade, D.O, *"Power Flow Analysis of the Nigerian Transmission System Incorporating Facts Controllers"*, International Journal of Applied Science and Technology, 2011.

[23] P R Sharma1 & Anirudh Dube, *"Location of SVC and UPFC for Real Power Loss Minimization and Stability Enhancement in a Multi Machine Power System using Parametric Approach"*, International Journal on Advanced Electrical and Electronics Engineering, 2012.

[24] BCP Busarello + Cott + Partner Inc., NEPLAN Planning and Optimization System for Electrical Network, http://www.neplan.ch.

[25] Dorin Bică, Cătălin Moldovan, Marius Muji, *"Power Engineering Education using NEPLAN software"*, Petru Maior University Publishing House, 2005.

APPENDICES

Appendix A: MATLAB program to carry out the line stability index using CPF function of MATPOWER.

```
clear
clc
define_constants;
mpcb = loadcase(sudan82);
mpopt = mpoption('pf.alg','NR','pf.tol',10^-3,
'pf.nr.max_it',50);
lampda=1.94;
%set up target case with
mpc = mpcb;
%increased generation
mpc.gen(:,[PG QG])=mpcb.gen(:,[PG QG])*lampda;
%increased load
mpc.bus(:,[PD QD])=mpcb.bus(:,[PD QD])*lampda;
Lmn=[];
results=runpf(mpc,mpopt);
X =mpc.branch(:,BR_X);
R =mpc.branch(:,BR_R);
Theta = atan(X./R);
Fbus =results.branch(:,F_BUS);
Tbus =results.branch(:,T_BUS);
VM =results.bus(:,VM);
Vangle =results.bus(:,VA);
Qr=results.branch(:,QT);
Qs=results.branch(:,QT);
for i=1:96
     Vs(i)=VM(Fbus(i));
     Ds(i)=Vangle(Fbus(i));
     Dr(i)=Vangle(Tbus(i));
     if Qr(i)<0
          Vs(i)=VM(Tbus(i));
          Ds(i)=Vangle(Tbus(i));
          Dr(i)=Vangle(Fbus(i));
          Qr(i)=abs(results.branch(i,QF));
          end
     end
D=((Ds-Dr)*pi/180)';
Vs=Vs';
lmn = (0.001*4.*X.*Qr)./(Vs.*sin(Theta-D)).^2;
Lmn=[Fbus Tbus lmn];
Lmn=Lmn(1:81,:);
```

Appendix B: Sudanese electrical network data.

Bus data:

Bus number	Type*	Pg	Qg	Pd	Qd	Bs	Base
		MW	MVAr	MW	MVAr	MVAr	KV
1	3	0	0	0	0	-125	500
2	1	0	0	0	0	-125	500
3	1	0	0	0	0	-250	500
4	1	0	0	0	0	0	500
5	1	0	0	14.36	11.483	-30	220
6	1	0	0	0	0	-40	220
7	1	0	0	33.456	23.961	0	220
8	1	0	0	0	0	0	220
9	1	0	0	50.32	46.148	0	220
10	1	0	0	29.808	20.496	0	220
11	1	0	0	0	0	0	220
12	1	0	0	101.338	70.734	0	220
13	1	0	0	33.264	20.615	0	220
14	1	0	0	0	0	0	220
15	1	0	0	0	0	0	220
16	1	0	0	0	0	0	220
17	1	0	0	13.574	8.661	0	220
18	2	186	0	0	0	0	220
19	1	0	0	0	0	0	220
20	1	0	0	60.883	37.732	0	220
21	1	0	0	0	0	0	220
22	1	0	0	0	0	0	220
23	1	0	0	14.112	8.746	0	220
24	1	0	0	0	0	0	220
25	1	0	0	0	0	0	220
26	1	0	0	0	0	0	220
27	1	0	0	6.989	25.534	0	220
28	2	85	0	46.704	32.357	0	220
29	1	0	0	16.464	8.842	0	220
30	1	0	0	12.029	5.585	0	220
31	2	148	0	8.333	5.76	-15	220
32	1	0	0	0.403	22.385	0	220
33	1	0	0	1.546	0.958	0	220
34	1	0	0	19.757	31.778	0	220
35	1	0	0	3.629	25.117	0	220
36	1	0	0	1.008	5.56	0	220
37	1	0	0	6.25	3.939	0	220
38	1	0	0	3.36	23.764	0	220
39	1	0	0	6.72	4.568	-15	220

40	1	0	0	3.36	2.503	0	220
41	1	0	0	0	0	-30	220
42	1	0	0	0	0	0	220
43	1	0	0	0.672	12.515	0	220
44	1	0	0	12.029	8.021	0	220
45	1	0	0	0	0	0	220
46	1	0	0	16.666	10.678	0	220
47	1	0	0	0	0	0	220
48	1	0	0	0	0	0	220
49	2	38	0	0	0	-30	220
50	1	0	0	81.917	53.127	0	110
51	1	0	0	68.006	39.992	0	110
52	1	0	0	41.328	17.854	0	110
53	2	76	0	0	0	0	110
54	1	0	0	44.621	20.718	0	110
55	1	0	0	74.189	46.562	0	110
56	1	0	0	12.634	8.128	15	110
57	1	0	0	50.266	33.255	0	110
58	1	0	0	17.203	8.477	0	110
59	1	0	0	40.387	18.165	0	110
60	1	0	0	85.344	58.018	0	110
61	1	0	0	64.915	40.06	0	110
62	1	0	0	75.466	42.566	0	110
63	1	0	0	59.069	30.588	0	110
64	1	0	0	81.312	54.43	0	110
65	1	0	0	0	0	0	110
66	1	0	0	0	0	0	110
67	1	0	0	36.49	24.236	0	110
68	1	0	0	0	0	0	110
69	1	0	0	0	0	0	110
70	1	0	0	24.73	12.738	0	110
71	1	0	0	11.088	5.864	0	110
72	1	0	0	27.821	14.253	0	110
73	1	0	0	56.717	26.986	0	110
74	1	0	0	10.886	4.058	0	110
75	1	0	0	0.336	1.476	0	110
76	1	0	0	0	0	0	110
77	1	0	0	7.594	4.037	0	110
78	2	7	0	4.704	2.238	0	110
79	1	0	0	14.381	9.552	0	110
80	1	0	0	11.021	6.539	0	110
81	1	0	0	18.614	12.315	0	110
82	2	2	0	15.254	8.604	0	66

*1 = PQ, 2 = PV, 3 = Slack

Line data:

From bus	To bus	R p.u.	X p.u.	B p.u.	rating MVA	ratio
67	69	0.086281	0.10438	9.81E-05	93.5	1
6	5	0.283781	1.279132	4.07E-02	213.84	1
11	10	0.054252	0.287679	4.74E-03	187	1
9	7	0.218861	1.16054	1.91E-02	187	1
12	13	0.096901	0.436777	5.56E-02	213.84	1
10	7	0.218421	1.158209	1.91E-02	187	1
11	8	0.272988	1.447553	2.38E-02	187	1
9	6	0.114897	0.461302	6.59E-02	275	1
9	8	0.218861	1.16054	1.91E-02	187	1
2	1	0.02651	0.261317	2.43E-01	1064	1
1	3	0.019376	0.190992	7.11E-01	1064	1
4	3	0.004122	0.040627	3.78E-02	1064	1
13	17	0.079597	0.319576	4.57E-02	275	1
18	17	0.003461	0.013895	1.99E-03	275	1
16	19	0.020764	0.093595	1.19E-02	213.84	1
52	51	0.030455	0.122273	1.09E-03	137.5	1
54	50	0.00886	0.03557	3.18E-04	137.5	1
53	52	0.033223	0.133388	1.19E-03	137.5	1
55	56	0.022149	0.088926	7.94E-04	137.5	1
54	53	0.00714	0.056157	3.25E-04	132	1
53	55	0.033223	0.133388	1.19E-03	137.5	1
14	20	0.014535	0.058357	8.34E-03	275	1
59	58	0.030455	0.122273	1.09E-03	137.5	1
58	57	0.03876	0.15562	1.39E-03	137.5	1
59	54	0.052488	0.228653	1.05E-03	85.8	1
59	60	0.008306	0.033347	2.98E-04	137.5	1
60	61	0.021595	0.086702	7.74E-04	137.5	1
61	62	0.030455	0.122273	1.09E-03	137.5	1
62	63	0.010521	0.04224	3.77E-04	137.5	1
64	63	0.016335	0.065583	5.86E-04	137.5	1
56	64	0.025748	0.10376	9.23E-04	137.5	1
65	63	0.045682	0.183409	1.64E-03	137.5	1
21	24	0.007851	0.041632	2.74E-03	187	1
24	23	0.025909	0.137386	9.05E-03	187	1
68	67	0.517686	0.626281	5.88E-04	31.57	1
59	68	0.287603	0.347934	3.27E-04	31.57	1
61	66	0.107975	0.433512	3.87E-03	137.5	1
23	22	0.024917	0.100041	1.43E-02	275	1
23	25	0.067521	0.358037	2.36E-02	187	1
69	71	2.214545	2.679091	2.52E-03	31.57	1
71	70	0.013843	0.055579	4.96E-04	137.5	1
71	72	0.041529	0.166736	1.49E-03	137.5	1
71	73	1.581818	1.913636	1.80E-03	31.57	1
22	27	0.10223	0.410447	5.87E-02	275	1
27	28	0.074198	0.297901	4.26E-02	275	1
25	26	0.043182	0.228977	1.51E-02	187	1
74	73	0.566653	1.559645	2.40E-03	55	1

26	29	0.06595	0.349711	2.30E-02	187	1
73	77	1.006612	1.217769	1.14E-03	31.57	1
77	78	1.72562	2.087603	1.96E-03	31.57	1
76	78	0.287603	0.347934	3.27E-04	31.57	1
75	76	2.760992	3.340165	3.14E-03	31.57	1
78	79	1.984463	2.400744	2.26E-03	31.57	1
73	80	2.041983	2.470331	2.32E-03	31.57	1
29	30	0.039256	0.208161	1.37E-02	187	1
30	31	0.139752	0.741054	4.88E-02	187	1
31	32	0.096901	0.38905	5.56E-02	275	1
30	33	0.062293	0.250103	3.57E-02	275	1
28	36	0.076829	0.308461	4.41E-02	275	1
35	34	0.174421	0.700289	2.50E-02	275	1
34	37	0.123202	0.494649	1.77E-02	275	1
37	38	0.091364	0.366818	1.31E-02	275	1
38	39	0.164731	0.661384	2.36E-02	275	1
39	40	0.10936	0.43907	1.57E-02	275	1
36	35	0.054195	0.21759	3.11E-02	275	1
28	32	0.11282	0.452965	6.47E-02	275	1
33	41	0.069215	0.277893	3.97E-02	275	1
42	46	0.065754	0.263998	3.77E-02	275	1
41	43	0.005707	0.022912	3.27E-03	275	1
43	42	0.04845	0.194525	2.78E-02	275	1
42	44	0.033825	0.135806	1.94E-02	275	1
46	45	0.030288	0.121606	1.74E-02	275	1
14	47	0.006229	0.02501	3.57E-03	275	1
47	15	0.01938	0.07781	1.11E-02	275	1
16	17	0.026302	0.105599	1.51E-02	275	1
43	48	0.01938	0.07781	1.11E-02	275	1
18	19	0.041529	0.166736	2.38E-02	275	1
19	21	0.00969	0.038905	5.56E-03	275	1
41	49	0.134277	0.539112	7.71E-02	275	1
81	80	4.400331	5.019917	5.21E-03	40.7	1
22	15	0.01938	0.087355	1.11E-02	213.84	1
25	70	0	0.511333	0	300	0.905
59	21	0	0.596	0	300	0.922
52	19	0	0.643333	0	450	0.905
12	2	0	0.393333	0	600	0.905
16	4	0	0.56	0	600	0.915
3	14	0	0.56	0	900	0.911
41	81	0	1.2	0	200	0.975
42	82	0	1.253	0	200	0.905
26	73	0	0.7045	0	200	0.918
69	23	0	1.34	0	150	0.905
29	76	0	1.424545	0	110	0.945
56	20	0	0.844667	0	450	0.975
15	65	0	0.858	0	300	0.925
1	11	0	0.243778	0	900	0.967
22	66	0	0.866667	0	150	0.913

MVAbase = 1000.